induced by immunization with type II collagen (CII), suggesting that V_α14 NKT cells are a potential target for RA therapy (5).

Although the precise function of V_α14 NKT cells remains to be elucidated, evidence indicates that V_α14 NKT cells play a critical role in the regulation of autoimmune responses (6–8). Abnormalities in the numbers and function of V_α14 NKT cells have been observed in patients with autoimmune diseases, including RA, as well as in a variety of mouse strains that are genetically predisposed to the development of autoimmune diseases (9–15). Despite these accumulating data, the role of V_α14 NKT cells in the pathogenesis of arthritis still remains unclear.

In the present study, we show that blockade of CD1d results in the amelioration of CIA. In addition, the severity of CIA induced in V_α14 NKT cell–deficient mice was reduced in comparison with that in wild-type mice, due to a reduction in the Th1 deviation of T cell responses to CII. Furthermore, mice deficient in V_α14 NKT cells were significantly less susceptible to antibody-induced arthritis, indicating that V_α14 NKT cells also contribute to autoantibody-mediated inflammation.

MATERIALS AND METHODS

Mice. DBA1/J mice were purchased from Oriental Yeast Co., Ltd (Tokyo, Japan). C57BL/6 (B6) mice were purchased from Clea Laboratory Animal Corporation (Tokyo, Japan). J_α281-knockout mice were kindly provided by Dr. Masaru Taniguchi (Riken Research Center for Allergy and Immunology, Yokohama, Japan) (16), and were generated in the 129 strain and backcrossed 10 times to the B6 background. CD1-knockout mice were kindly provided by Dr. Steve B. Balk (Beth Israel Deaconess Medical Center, Harvard Medical School, Boston, MA) (17), and were generated in the 129 strain and backcrossed 7 times to the B6 background. KRN TCR–transgenic mice were kindly provided by Drs. Christophe Benoist and Diane Mathis (Joslin Diabetes Center, Boston, MA) (18). The animals were kept under specific pathogen–free conditions.

Flow cytometric analysis of NKT cells. Cells were prepared from various organs of control DBA1/J mice and CIA mice at 30–35 days after the first immunization. Control mice were injected intradermally with vehicle alone emulsified in Freund's complete adjuvant (CFA) at day 0 and in Freund's incomplete adjuvant (IFA) at day 21. Dimer XI Recombinant Soluble Dimetric Mouse CD1d, fluorescein isothiocyanate–conjugated A85-1 monoclonal antibodies (mAb) (anti-mouse IgG1), and allophycocyanin-conjugated anti-TCRβ chain were purchased from BD Biosciences PharMingen (San Diego, CA). Loading of α-GC to CD1d and staining for Dimer XI were achieved in accordance with the manufacturer's protocol. Flow cytometric analysis was performed with FACSCaliber flow cytometry (Becton Dickinson Immunocytometry Systems, Mountain View, CA).

Induction of CIA. Mice were immunized intradermally at the base of the tail with either 200 μg of bovine CII (for DBA1/J mice) or 100 μg of chicken CII (for B6 mice) (Collagen Research Center, Tokyo, Japan) emulsified with an equal volume of CFA and containing 250 μg of H37Ra *Mycobacterium tuberculosis* (Difco, Detroit, MI). B6 mice received a booster by intradermal injection with the same antigen preparation on day 21. DBA1/J mice received a booster by intradermal injection with 200 μg of bovine CII emulsified with IFA.

Induction of anti-CII antibody–induced arthritis. Mice were injected intravenously with 2 mg of the mixture of anti-CII mAb (Arthrogen-CIA mAb; Chondrex, Seattle, WA), and 3 days later, 50 μg of lipopolysaccharide (LPS) was injected intraperitoneally. Control mice were injected with mouse IgG (Sigma, St. Louis, MO) followed by LPS injection.

Induction of arthritis by K/BxN serum transfer. As previously described, KRN TCR–transgenic mice maintained on the B6 background were crossed with nonobese diabetic (NOD) mice to generate K/BxN mice that develop spontaneous arthritis (18). K/BxN serum pools were prepared from 8-week-old, arthritic mice, and 200 μl of the serum was injected intraperitoneally into the animals to induce arthritis. Sera from nontransgenic littermate mice crossed with NOD mice (BxN) were used as the control.

Clinical assessment of arthritis. Mice were examined for signs of joint inflammation, using the following scoring system: 0 = no change, 1 = significant swelling and redness of 1 digit, 2 = mild swelling and erythema of the limb or swelling of >2 digits, 3 = marked swelling and erythema of the limb, and 4 = maximal swelling and redness of the limb and subsequent ankylosis. The average of the macroscopic score was expressed as the cumulative value of all paws, with a maximum possible score of 16.

In vivo antibody treatment. Anti-CD1–blocking, non–cell-depleting mAb (1B1) was purchased from BD Biosciences PharMingen (19). Mice were treated intraperitoneally with 250 μg of either blocking anti-CD1d mAb or non–isotype-matched whole rat IgG (Sigma) as control, twice per week starting from 21 days after the first immunization with CII.

Measurements of CII-specific IgG1 and IgG2a. Either chicken or bovine CII (1 mg/ml) was coated onto enzyme-linked immunosorbent assay plates (Sumitomo Bakelite, Tokyo, Japan) at 4°C overnight. After blocking with 1% bovine serum albumin in phosphate buffered saline, serially diluted serum samples were added to CII-coated wells. For detection of anti-CII antibodies, the plates were incubated for 1 hour with biotin-labeled anti-IgG1 and anti-IgG2a (Southern Biotechnology Associates, Birmingham, AL) or anti-IgG antibodies (CN/Cappel, Aurora, OH) and then incubated with streptavidin-peroxidase. After adding a substrate, the reaction was evaluated, and antibody titers were calculated on the basis of dilution/absorbance curves.

Cytokine measurement. B6 or J_α281-knockout mice were immunized with 100 μg of CII on days 0 and 21. Ten days after the second immunization, the lymph node cells from B6 or J_α281-knockout mice were cultured for 48 hours with 200 μg/ml CII. The levels of IL-2, IL-4, IL-5, IL-10, IFNγ, and tumor necrosis factor α (TNFα) in the supernatants were measured by cytometric bead array (BD PharMingen), using the protocol provided by the manufacturer.

Histopathology. B6 or J_α281-knockout mice were killed and the fore paws removed 65 days after the induction of CIA or 10 days after K/BxN serum transfer. Paws were then fixed in buffered formalin, decalcified, embedded in paraffin, sectioned, and stained with hematoxylin and eosin.

RESULTS

Increase in liver NKT cells in CIA. To investigate the role of CD1-restricted V_α14 NKT cells in CIA, we first analyzed the number of V_α14 NKT cells using α-GC–loaded CD1 dimer. As shown in Figure 1A, the percentage of α-GC–loaded CD1-reactive V_α14 NKT cells among total liver mononuclear cells and peripheral blood mononuclear cells (PBMCs) was increased in CIA mice compared with control mice treated with CFA alone. The absolute number of α-GC–loaded CD1-reactive V_α14 NKT cells was also increased in the liver at the peak of the disease (Figure 1B).

Amelioration of CIA by anti-CD1 mAb treatment. To elucidate the role of V_α14 NKT cells in the pathogenesis of arthritis, we next examined the effect of anti-CD1d mAb on the development of CIA. We immunized DBA1/J mice and then administered intraperitoneal injections of either anti-CD1d mAb or control rat IgG twice per week starting from the day of the second immunization (5). As shown in Figure 2A, anti-CD1d treatment ameliorated arthritis in the mAb treatment

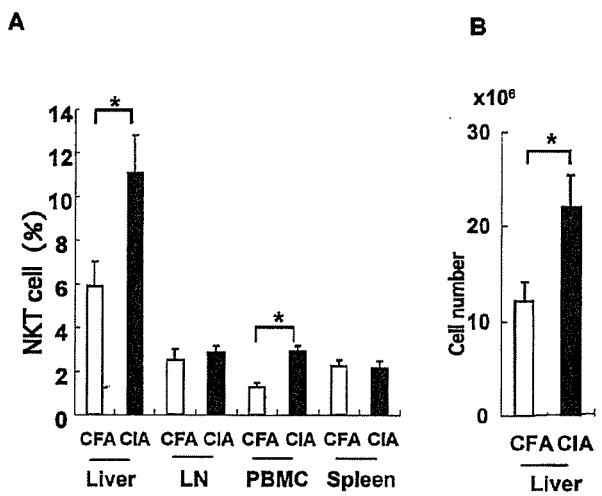

Figure 1. Expression of natural killer T (NKT) cells in the collagen-induced arthritis (CIA) model. **A,** To determine the frequency of NKT cells in various organs of mice with CIA or control mice (treated with Freund's complete adjuvant [CFA]), cells were obtained from the mice at the time of death, 30–35 days after the first immunization. Results are expressed as the percentage of α-galactosylceramide–loaded CD1d-positive T cells within the lymphocyte gates. LN = lymph nodes; PBMC = peripheral blood mononuclear cells. **B,** Absolute numbers of NKT cells in the liver were calculated from the total liver mononuclear cells of the same mice as in A. Bars show the mean and SEM of 7–8 mice per group. * = $P < 0.05$, by Mann-Whitney U test.

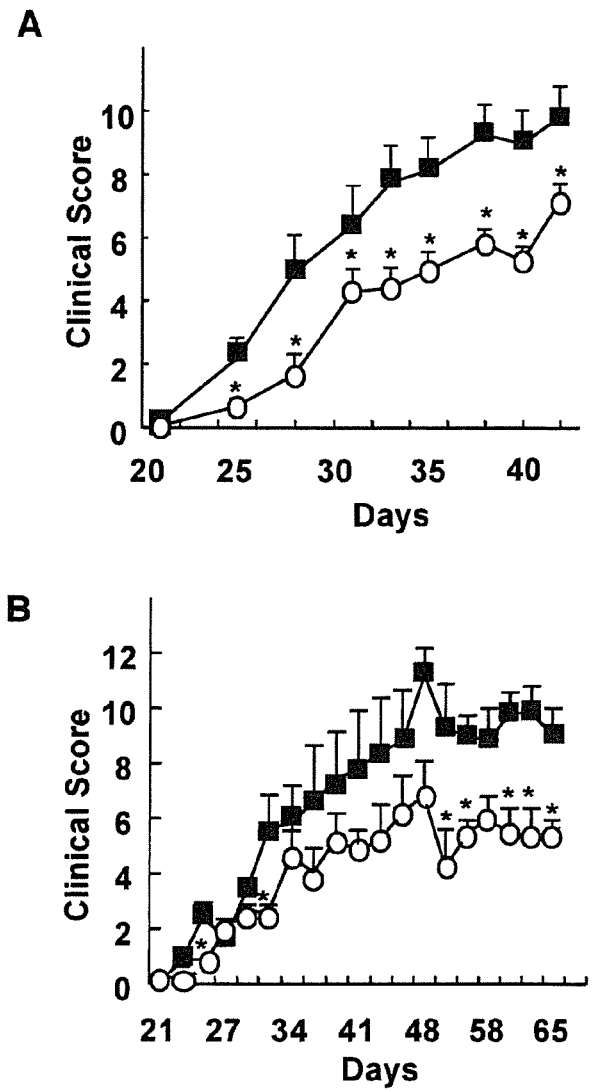

Figure 2. Amelioration of collagen-induced arthritis (CIA) in **A,** anti-CD1 monoclonal antibody (mAb)–treated or **B,** natural killer T cell–deficient mice. **A,** The clinical course of CIA was monitored in DBA/1 mice treated with 250 μg of anti-CD1d mAb (○) or control rat IgG (■), twice per week starting from day 21 after the first immunization. Bars show the mean and SEM of 13 mice (6-week-old males) per group from 2 independent experiments (n = 5 or 8 per group). * = $P < 0.05$ versus control IgG-treated mice, by Mann-Whitney U test. **B,** The clinical course of CIA was monitored in J_α281-knockout (○) and wild-type B6 (■) mice immunized with chicken type II collagen emulsified with Freund's complete adjuvant. Bars show the mean and SEM of 5 mice per group. * = $P < 0.05$ versus B6 mice, by Mann-Whitney U test.

group as compared with that in the control group. Disease susceptibility was not different between anti-CD1d–treated mice and control mice. This result suggests that CD1d-restricted $V_\alpha 14$ NKT cells contribute to the enhancement of the disease course in CIA.

Reduced severity of CIA in NKT cell–deficient mice. To further investigate the contribution of CD1-restricted $V_\alpha 14$ NKT cells to arthritis, we induced CIA in $V_\alpha 14$ NKT cell–deficient $J_\alpha 281$-knockout mice. As shown in Figure 2B, $V_\alpha 14$ NKT cell–deficient mice developed less severe arthritis compared with that in the wild-type B6 mice. Disease susceptibility was not different between B6 mice and $J_\alpha 281$-knockout mice. This result further supports the idea that $V_\alpha 14$ NKT cells could play a role in the enhancement of CIA.

Altered CII-specific responses in NKT cell–deficient mice. To examine whether the response to CII was altered in the presence or absence of $V_\alpha 14$ NKT cells, we measured CII-specific IgG isotype levels 65 days after the induction of CIA. It is generally accepted that elevation of autoantigen-specific IgG2a antibody is the result of augmentation of the Th1 immune response to the antigen, whereas a higher level of IgG1 antibody is a reflection of a stronger Th2 response to the antigen. In $J_\alpha 281$-knockout mice, there was a slight reduction in the level of antigen-specific IgG2a antibody and an increase in the level of antigen-specific IgG1 compared with that in wild-type B6 mice (Figure 3A). Consequently, the IgG1:IgG2a ratio was elevated in $J_\alpha 281$-knockout mice, suggesting that $V_\alpha 14$ NKT cell deficiency alters the Th1/Th2 balance in response to CII.

To further analyze the CII-reactive T cell response, we isolated the draining lymph node cells from B6 or $J_\alpha 281$-knockout mice 10 days after the second immunization with CII, and stimulated the lymphoid cells with CII in vitro. We then compared the concentrations of IL-2, IL-4, IL-5, IL-10, IFNγ, and TNFα in the culture supernatants. The level of IL-10 was significantly increased in the supernatant obtained from the culture of lymphoid cells of $J_\alpha 281$-knockout mice compared with those from B6 mice (Figure 3B). The concentrations of IL-2 and IFNγ were decreased in $J_\alpha 281$-knockout mice; however, the levels of these cytokines were also very low in B6 mice. The concentration of TNFα was not different between these mice. IL-4 and IL-5 were not detected in either culture supernatant. These results suggest that $V_\alpha 14$ NKT cells contribute to the alteration of the Th1/Th2 balance of the T cell response to CII.

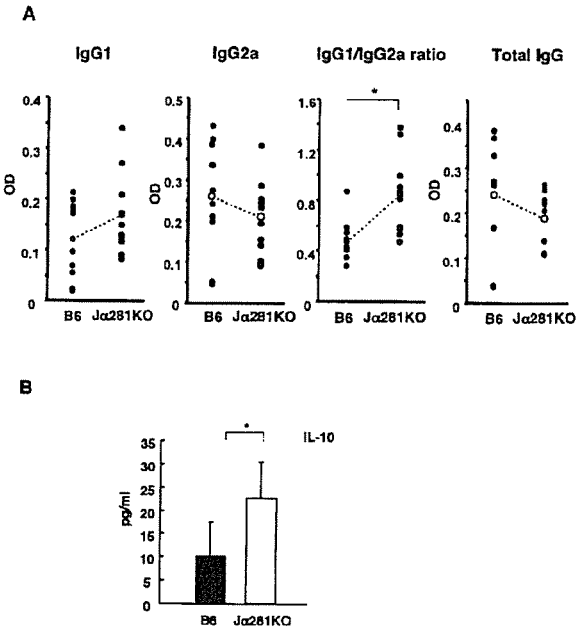

Figure 3. Altered type II collagen (CII)–specific responses in natural killer T cell–deficient mice. **A**, To determine the CII-specific antibody isotype levels in $J_\alpha 281$-knockout (Jα281KO) mice as compared with wild-type B6 mice, individual serum samples obtained on day 65 after induction of arthritis were analyzed by enzyme-linked immunosorbent assay, with results expressed as the optical density (OD). Open circles with broken lines denote the average of individual samples. * = $P < 0.05$, by Student's *t*-test. **B**, To determine the CII-specific T cell response in Jα281KO as compared with wild-type B6 mice, production of interleukin-10 (IL-10) (among other cytokines) from draining lymph node cells was analyzed by cytometric bead array. Bars show the mean and SEM of 3 mice per group. * = $P < 0.05$, by Mann-Whitney U test.

Amelioration of antibody-induced arthritis in NKT cell–deficient mice. CIA, commonly used as a model of RA, is characterized both by a primary immune response and by inflammation, and these features are often interdependent and therefore difficult to separate. In antibody-induced arthritis, inflammation occurs in the absence of a primary immune response, allowing us to investigate the effector mechanisms that link the potentially pathogenic antibodies and the overt development of arthritis (20). To address the role of $V_\alpha 14$ NKT cells in the inflammatory process in addition to the modulation of the T cell response, we studied the role of $V_\alpha 14$ NKT cells in anti-CII antibody–induced arthritis. To induce arthritis, mice received a mixture of 4 mAb reactive to CII, followed 72 hours later by LPS. As shown in Figure 4, compared with that in control animals, the severity of joint inflammation was signifi-

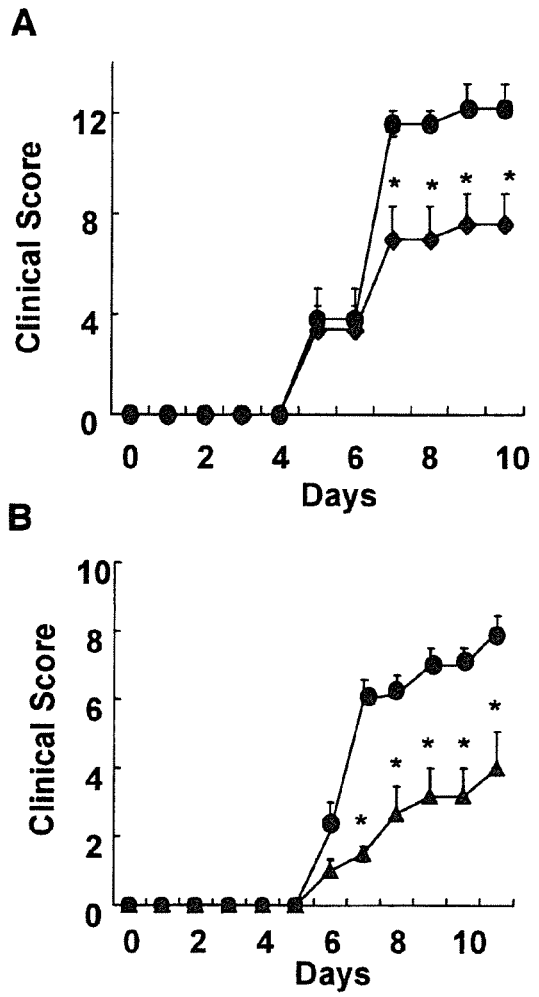

Figure 4. Reduced severity of anti–type II collagen monoclonal antibody (anti-CII mAb)–induced arthritis in natural killer T cell–deficient mice. The clinical course of arthritis induced by injection of a mixture of anti-CII mAb and lipopolysaccharide was monitored in 7-week-old female **A**, J_α281-knockout mice (◆) and **B**, CD1-knockout mice (▲) as compared with B6 mice (● in **A** and **B**). Bars show the mean and SEM of 5 mice per group, with representative data from 1 of 2 experiments. * = $P < 0.05$ versus B6 mice, by Mann-Whitney U test.

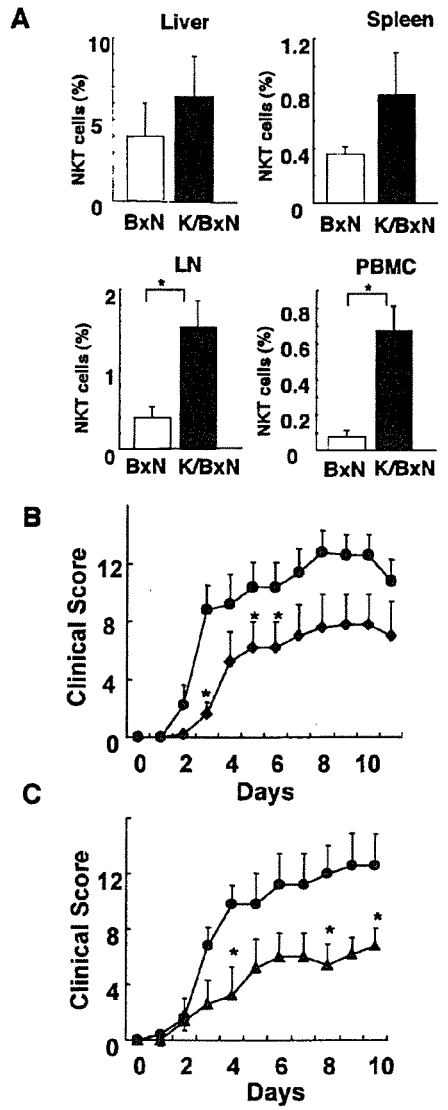

Figure 5. Reduced severity of arthritis induced by transfer of K/BxN serum in natural killer T (NKT) cell–deficient mice. **A**, To determine the frequency of NKT cells in various organs of mice with K/BxN serum–induced arthritis or BxN serum–transferred control mice, cells were obtained from the mice at the time of death, 10 days after serum transfer. Results are expressed as the percentage of α-galactosylceramide–loaded CD1-positive T cells within the lymphocyte gates. Bars show the mean and SEM of 3 mice per group. * = $P < 0.05$, by Mann-Whitney U test. LN = lymph nodes; PBMC = peripheral blood mononuclear cells. **B** and **C**, The clinical course of arthritis induced by the injection of K/BxN serum was monitored in 8-week-old female **B**, J_α281-knockout mice (◆) and **C**, CD1-knockout mice (▲) as compared with B6 mice (● in **B** and **C**). Bars show the mean and SEM of 5 mice per group, with representative data from 1 of 2 experiments. * = $P < 0.05$, by Mann-Whitney U test.

cantly reduced in J_α281-knockout mice as well as in CD1d-knockout mice, another NKT cell–deficient type of mouse (17). Disease susceptibility was not different among these 3 groups.

Arthritis induced by K/BxN serum transfer is another antibody-induced arthritis model (21). K/BxN is a recently developed model of inflammatory arthritis (18). K/BxN animals spontaneously develop arthritis

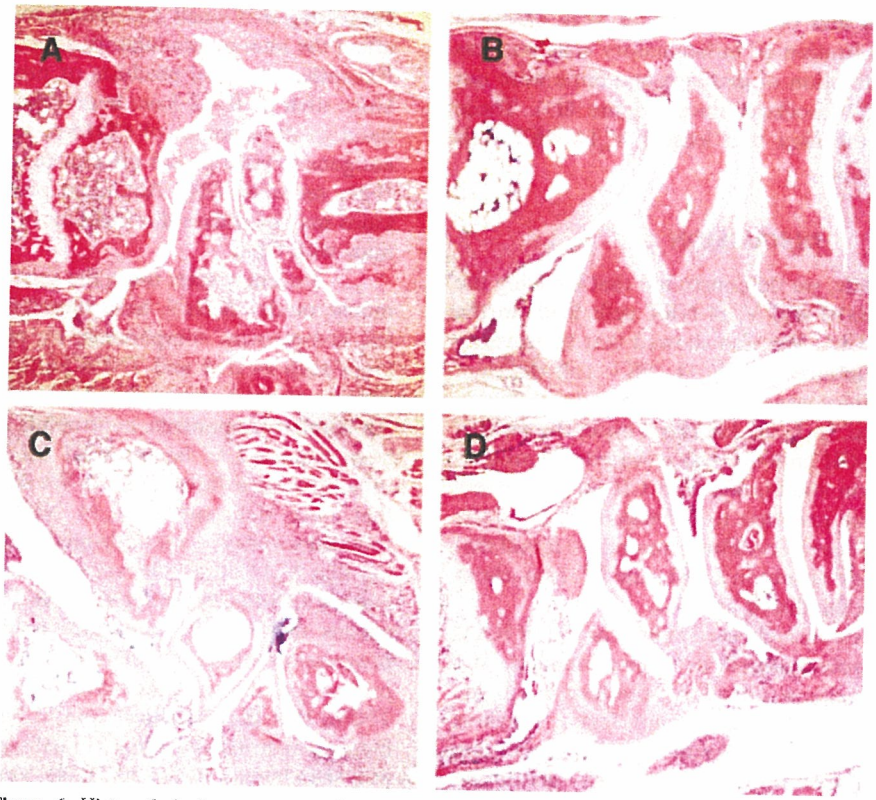

Figure 6. Histopathologic assessment of arthritic wrist joints. The joints from B6 mice and $J_{\alpha}281$-knockout mice with collagen-induced arthritis (**A** and **B**, respectively) and from B6 mice and $J_{\alpha}281$-knockout mice with K/BxN serum–transferred arthritis (**C** and **D**, respectively) were assessed for the extent of arthritis. Two mice per group were analyzed, and representative results are shown. (Hematoxylin and eosin stained; original magnification × 20.)

that is similar to RA in humans. The arthritis is initiated by T and B cell autoreactivity to a ubiquitously expressed antigen, glucose-6-phosphate-isomerase (GPI) (22). Transfer of serum from arthritic K/BxN mice into healthy animals provokes arthritis within days, independent of the response of T and B cells. K/BxN serum–induced arthritis is mediated by anti-GPI IgG.

With this arthritis model, we analyzed the number of $V_{\alpha}14$ NKT cells, utilizing α-GC–loaded CD1 dimer. As shown in Figure 5A, the percentage of α-GC–loaded CD1-restricted $V_{\alpha}14$ NKT cells among lymph node cells and PBMCs in arthritic mice was increased compared with that in control mice transferred with BxN serum. CD1-restricted $V_{\alpha}14$ NKT cells among total liver mononuclear cells and splenocytes tended to be increased in arthritic mice. As shown in Figures 5B and C, the severity of joint inflammation was significantly reduced in $J_{\alpha}281$-knockout mice and CD1d-knockout mice, respectively, as compared with that in control animals, which is consistent with the results observed in anti-CII antibody–induced arthritis. Disease susceptibility was not different among these 3 groups. These results indicate that $V_{\alpha}14$ NKT cells contribute to the inflammatory effector phase of arthritis.

Histopathologic assessment of arthritis in $J_{\alpha}281$-knockout mice. In addition to visual scoring of disease severity, we analyzed the histologic features in the joints of the fore paws of $J_{\alpha}281$-knockout mice and wild-type B6 mice on day 65 after CIA induction or 10 days after K/BxN serum transfer. As shown in Figure 6A, following arthritis development in B6 mice, there was severe disease in the joints, associated with massive cell infiltration, cartilage erosion, and bone destruction. These histologic features were significantly less apparent in $J_{\alpha}281$-knockout mice (Figure 6B). In K/BxN serum–transferred B6 mice, massive cell infiltration as well as

cartilage erosion and bone destruction were observed (Figure 6C). Infiltration of inflammatory cells was less evident and destruction of cartilage and bone were not apparent in J_α281-knockout mice (Figure 6D). These results support the idea that loss of V_α14 NKT cells ameliorates arthritis.

DISCUSSION

In this study, we demonstrated that blocking the interaction of CD1d and V_α14 NKT cells leads to the amelioration of CIA. We also showed that the severity of the disease induced in V_α14 NKT cell–deficient J_α281-knockout mice was reduced compared with that in wild-type B6 mice. In J_α281-knockout mice, the ratio of IgG1:IgG2a anti-CII antibody was elevated and production of IL-10 upon stimulation with CII was increased, suggesting that the response to CII was deviated to the Th2 response in these mice. Furthermore, we found that the disease was less severe in J_α281- and CD1-knockout mice with antibody-induced arthritis.

The most extensively used animal model of RA is CIA, which is accompanied by a predominant Th1 response and is characterized by production of the proinflammatory cytokines IFNγ and TNFα. Previous studies have shown that treatment with Th2-promoting cytokines or with mAb directed against Th1-promoting cytokines can effectively protect mice against CIA (23). V_α14 NKT cells were previously reported to protect other Th1 cell–mediated autoimmune diseases such as type I diabetes in NOD mice, by inducing a shift toward a Th2 T cell response to autoantigens (6–8). The development of diabetes was prevented either by infusion of NKT cell–enriched thymocyte preparations or by an increase of NKT cells in V_α14–J_α281–transgenic NOD mice (24,25). In contrast, V_α14 NKT cells appeared to exacerbate arthritis in the present study, since the severity of the disease was decreased in J_α281-knockout mice and anti-CD1d mAb treatment ameliorated the disease.

Because V_α14 NKT cells produce large amounts of both IL-4 and IFNγ upon stimulation with anti-CD3 antibody or its prototypic ligand α-GC, a regulatory role in Th cell differentiation has been proposed for these cells. However, the results obtained from α-GC treatment of B6 mice on Th cell differentiation are conflicting. The administration of α-GC was found to facilitate either Th1 differentiation or Th2 differentiation (26,27). Although the basis for these inconsistencies is not clear, the discrepancies between these results could be due to the differences in the protocols of the α-GC treatment, suggesting that small differences in circumstances may affect the immunomodulatory effect of V_α14 NKT cells. Recently, microbial products or proinflammatory cytokines such as IL-12 have been reported to amplify the basal weak responses of CD1d-restricted T cells to self antigens to yield potent effector functions by enhancing IFNγ secretion (28). Abundant proinflammatory cytokines may modulate the function of V_α14 NKT cells in mice with CIA.

Recent studies using the serum of an engineered mouse model, K/BxN, have revealed that autoantibodies, complement components, Fc receptors, and cytokines such as IL-1 and TNFα participate in the pathogenesis of antibody-mediated erosive arthritis (29–31). As cellular components, neutrophils and mast cells have been reported to be essential for antibody-mediated inflammatory arthritis (32,33). We showed, in this study, that mice deficient in V_α14 NKT cells exhibited a reduced severity of antibody-mediated arthritis, suggesting that V_α14 NKT cells act as effector cells in inflammatory arthritis. Potential V_α14 NKT cell effector mechanisms that may be important for the induction and progression of joint inflammation include the rapid production of a variety of cytokines, including IL-1 and TNFα, that play a critical role in both K/BxN serum–induced arthritis and anti-CII mAb–induced arthritis, as well as in human RA (1,30,31,34). Very recently, Kim et al reported that NKT cells promote K/BxN serum–induced joint inflammation by producing IL-4 and IFNγ (35). Those authors showed that IL-4 and IFNγ are important in reducing the production of transforming growth factor β (TGFβ), resulting in suppression of arthritis. The regulation of TGFβ by NKT cells might be one of the important mechanisms controlling the inhibition of arthritis.

In this study we have demonstrated that V_α14 NKT cells could contribute to the pathogenesis of arthritis in several ways, including enhancing the inflammatory effector phase of arthritis mediated by autoantibodies. Changing the Th1/Th2 balance of autoantigen-reactive T cells by V_α14 NKT cells may also contribute to the pathogenesis of CIA. As we previously proposed, modulation of the function of V_α14 NKT cells with proper stimuli, such as the Th2-skewing glycolipid ligand, OCH, or a blocking reagent for NKT cell functions, could be considered as new therapeutic interventions in the management of RA.

ACKNOWLEDGMENTS

We thank Masaru Taniguchi at the Riken Research Center for Allergy and Immunology for providing the J_α281-

knockout mice, Steven Balk at Beth Israel Deaconess Medical Center and Harvard Medical School for providing the CD1-knockout mice, and Drs. Christophe Benoist and Diane Mathis, Joslin Diabetes Center and Harvard Medical School and Institu de Genetique et de Biologie Moleculaire et Cellulaire for providing the TCR-transgenic mice. We also thank Miho Mizuno and Chiharu Tomi for excellent technical assistance. We are grateful to John Ludvic Croxford for critical reading of the manuscript.

REFERENCES

1. Feldmann M, Brennan FM, Maini RN. Role of cytokines in rheumatoid arthritis. Annu Rev Immunol 1996;14:397–440.
2. Brenner MB, Brigl M. CD1: antigen presentation and T cell function. Annu Rev Immunol 2004;22:817–90.
3. Taniguchi M, Harada M, Kojo S, Nakayama T, Wakao H. The regulatory role of Vα14 NKT cells in innate and acquired immune response. Annu Rev Immunol 2003;21:483–513.
4. Kronenberg M, Gapin L. The unconventional lifestyle of NKT cells. Nat Rev Immunol 2002;2:557–68.
5. Chiba A, Oki S, Miyamoto K, Hashimoto H, Yamamura T, Miyake S. Suppression of collagen-induced arthritis by natural killer T cell activation with OCH, a sphingosine-truncated analog of α-galactosylceramide. Arthritis Rheum 2004;50:305–13.
6. Hammond KJ, Godrey DI. NKT cells: potential targets for autoimmune disease therapy? Tissue Antigens 2002;59:353–63.
7. Wilson SB, Delovitch TL. Janus-like role of regulatory iNKT cells in autoimmune disease and tumour immunity. Nat Rev Immunol 2003;3:211–22.
8. Hammond KJ, Kronenberg M. Natural killer T cells: natural or natural regulators of autoimmunity? Curr Opin Immunol 2003;15: 683–9.
9. Sumida T, Sakamoto A, Murata H, Makino Y, Takahashi H, Yoshida S, et al. Selective reduction of T cells bearing invariant Vα24JαQ antigen receptor in patients with systemic sclerosis. J Exp Med 1995;182:1163–8.
10. Wilson SB, Kent SC, Patton KT, Orban T, Jackson RA, Exley M, et al. Extreme Th1 bias of invariant Vα24JαQ T cells in type 1 diabetes. Nature 1998;391:177–81.
11. Illes Z, Kondo T, Newcombe J, Oka N, Tabira T, Yamamura T. Differential expression of NK T cell Vα24JαQ invariant TCR chain in the lesions of multiple sclerosis and chronic inflammatory demyelinating polyneuropathy. J Immunol 2000;164:4375–81.
12. Kojo S, Adachi Y, Keino H, Taniguchi M, Sumida T. Dysfunction of T cell receptor AV24AJ18+, BV11+ double-negative regulatory natural killer T cells in autoimmune diseases. Arthritis Rheum 2001;44:1127–38.
13. Yoshimoto T, Bendelac A, Hu-Li J, Paul WE. Defective IgE production by SJL mice is linked to the absence of CD4+, NK1.1+ T cells that promptly produce interleukin 4. Proc Natl Acad Sci U S A 1995;92:11931–4.
14. Mieza MA, Itoh T, Cui JQ, Makino Y, Kawano T, Tsuchida K, et al. Selective reduction of Vα14+ NK T cells associated with disease development in autoimmune-prone mice. J Immunol 1996;156:4035–40.
15. Gombert JM, Herbelin A, Tancrede-Bohin E, Dy M, Carnaud C, Bach JF. Early quantitative and functional deficiency of $NK1^+$-like thymocytes in the NOD mouse. Eur J Immunol 1996;26:2989–98.
16. Cui J, Shin T, Kawano T, Sato H, Kondo E, Toura I, et al. Requirement for Vα14 NKT cells in IL-12-mediated rejection of tumors. Science 1997;278:1623–6.
17. Sonoda KH, Exley M, Snapper S, Balk SP, Stein-Streilein J. CD1-reactive natural killer T cells are required for development of systemic tolerance through an immune-privileged site. J Exp Med 2003;3:211–22.
18. Kouskoff V, Korganow AS, Duchatelle V, Degott C, Benoist C, Mathis D. Organ-specific disease provoked by systemic autoimmunity. Cell 1996;87:811–22.
19. Szalay G, Ladel CH, Blum C, Brossay L, Kronenberg M, Kaufmann SH. Anti-CD1 monoclonal antibody treatment reverses the production patterns of TGF-β2 and Th1 cytokines and ameliorates listerosis in mice. J Immunol 1999;162:6955–8.
20. Terato K, Hasty KA, Reife RA, Cremer MA, Kang H, Stuart JM. Induction of arthritis with monoclonal antibodies to collagen. J Immunol 1992;148:2103–8.
21. Korganow AS, Ji H, Mangialaio S, Dchatelle V, Pelanda R, Martin T, et al. From systemic T cell self-reactivity to organ-specific autoimmune disease via immunoglobulins. Immunity 1999;10: 451–61.
22. Matsumoto I, Staub A, Benoist C, Mathis D. Arthritis provoked by linked T and B cell recognition of a glycolytic enzyme. Science 1999;286:1732–5.
23. Van Roon JA, Lafeber FP, Bijlsma JW. Synergistic activity of interleukin-4 and interleukin-10 in suppression of inflammation and joint destruction in rheumatoid arthritis [review]. Arthritis Rheum 2001;44:3–12.
24. Hammond KJ, Poulton LD, Palmisano LJ, Silveria PA, Godfrey DJ, Baxter AG. α/β-T cell receptor+CD4−CD8− (NKT) thymocytes prevent insulin-dependent diabetes mellitus in nonobese diabetic (NOD)/Lt mice by the influence of interleukin (IL)-4 and/or IL-10. J Exp Med 1998;187:1047–56.
25. Lehuen A, Lantz O, Beaudoin L, Laloux V, Carnaud C, Bendelac A, et al. Overexpression of natural killer T cells protects Vα14-Jα281 transgenic nonobese diabetic mice against diabetes. J Exp Med 1998;188:1831–9.
26. Singh N, Hong S, Scherer DC, Serizawa I, Burdin N, Kronenberg M, et al. Activation of NKT cells by CD1d and α-galactosylceramide directs conventional T cells to the acquisition of a Th2 phenotype. J Immunol 1999;163:2373–7.
27. Cui J, Watanabe N, Kawano T, Yamashita M, Kamata T, Shimizu C, et al. Inhibition of T helper cell type 2 cell differentiation and immunoglobulin E response by ligand-activated Vα14 natural killer T cells. J Exp Med 1999;190:783–92.
28. Brigl M, Bry L, Kent SC, Gumperz JE, Brenner MB. Mechanism of CD1d-restricted natural killer T cell activation during microbial infection. Nat Immunol 2003;12:1230–7.
29. Ji H, Ohmura K, Mahmood U, Lee DM, Hofhuis FM, Boackle SA, et al. Arthritis critically dependent on innate immune system players. Immunity 2002;16:157–68.
30. Kagari T, Doi H, Shimozato T. The importance of IL-1β and TNF-α, and the noninvolvement of IL-6, in the development of monoclonal antibody-induced arthritis. J Immunol 2002;169: 1459–66.
31. Ji H, Pettit A, Ohmura K, Ortiz-Lopez A, Duchatelle V, Degott C, et al. Critical roles for interleukin 1 and tumor necrosis factor α in antibody-induced arthritis. J Exp Med 2002;196:77–85.
32. Wipke BT, Allen PM. Essential role of neutrophils in the initiation and progression of a murine model of rheumatoid arthritis. J Immunol 2001;167:1601–8.
33. Lee DM, Friend DS, Gurish MF, Benoist C, Mathis D, Brenner MB. Mast cells: a cellular link between autoantibodies and inflammatory arthritis. Science 2002;297:1689–92.
34. Oki S, Chiba A, Yamamura T, Miyake S. The clinical implication and molecular mechanism of preferential IL-4 production by modified glycolipid-stimulated NKT cells. J Clin Invest 2004;113: 1631–40.
35. Kim HY, Kim HJ, Min HS, Kim S, Park WS, Park SH, et al. NKT cells promote antibody-induced joint inflammation by suppressing transforming growth factor β1 production. J Exp Med 2005;201: 41–7.

Single Dose of OCH Improves Mucosal T Helper Type 1/T Helper Type 2 Cytokine Balance and Prevents Experimental Colitis in the Presence of Vα14 Natural Killer T Cells in Mice

Yoshitaka Ueno, MD, Shinji Tanaka, MD, PhD,* Masaharu Sumii, MD, PhD,† Sachiko Miyake, MD, PhD,‡ Susumu Tazuma, MD, PhD,† Masaru Taniguchi, MD, PhD,§ Takashi Yamamura, MD, PhD,‡ and Kazuaki Chayama, MD, PhD†*

Background and Aims: Vα14 natural killer T (NKT) cells seem to play important roles in the development of various autoimmune diseases. However, the pathophysiologic role of NKT cells in inflammatory bowel disease remains unclear. To clarify the mechanism by which the activation of NKT cells mediates protection against intestinal inflammation, we investigated the antiinflammatory role of specifically activated Vα14 NKT cells by glycolipids in a mouse experimental model of colitis induced by dextran sulfate sodium (DSS).

Methods: Colitis was induced in C57BL/6 mice by the oral administration of 1.5% DSS for 9 days. A single dose of OCH or α-galactosylceramide, a ligand for NKT cells, was administered on day 3 after the induction of colitis. Body weights and colonic mucosal injury were assessed in each glycolipid-treated group. Interferon-γ and interleukin-4 levels in the supernatants from colonic lamina propria lymphocytes (LPLs) were measured by enzyme-linked immunosorbent assay.

Results: The administration of a single dose of OCH attenuated colonic inflammation, as defined by body weights and histologic injury. The protective effects of OCH could not be observed in Vα14 NKT cell-deficient mice. In vivo treatment with OCH had improved the interferon-γ/interleukin-4 ratio from colonic LPLs on day 9 after DSS treatment.

Conclusion: The present data indicated that the activation of Vα14 NKT cells by OCH plays a pivotal role in mediating intestinal inflammation via altered mucosal T-helper type 1/type 2 responses. Therapeutic strategies that are designed to activate specifically Vα14 NKT cells may prove to be beneficial in treating intestinal inflammation.

Key Words: colitis, natural killer T cells, OCH, T helper type 1/T helper type 2

(*Inflamm Bowel Dis* 2005;11:35–41)

Natural killer T (NKT) cells have been identified as a novel lymphoid lineage distinct from conventional T cells and natural killer (NK) cells. NKT cells express both invariant Vα14 NKT-specific antigen receptor as well as an NK marker (NK1.1).[1–5] The specific features of this cell type include a limited repertoire with an invariant Vα chain consisting of the Vα14-Jα281 gene segment and the highly skewed Vβ chains Vβ8.2, Vβ7, and Vβ2 in mice. NKT cells are restricted by the nonclassical major histocompatibility complex class I-like molecule CD1d, which is expressed on cells of hematopoietic origin as well as on intestinal epithelial cells.[6–10] These cells recognize glycolipid antigens such as α-galactosylceramide (αGalCer), a glycolipid that is isolated from marine sponges that specifically binds CD1d.[11–14] NKT cells are abundant in the thymus, liver, and bone marrow, and are also found in peripheral lymphoid organs. It has been reported that NKT cells play an important role in various aspects of the immune response, including the regulation of allergic and autoimmune diseases[15–18] and the prevention of tumor metastasis.[19–22]

One of the mechanisms by which NKT cells elicit the effector function is through the production of large amounts of interferon (IFN)-γ, interleukin (IL)-4, and IL-10 in response to various stimuli.[1] In vitro and in vivo studies have shown that the cytokine profiles of these cells depend both on the nature of the activating stimulus and on the nature of the cytokines, and on other soluble factors in the local microenvironment. The activation of $NK1.1^+$T cells by CD3 cross-linking or CD1 results in the production of both IFN-γ and IL-4, whereas the stimulation of $NK1.1^+$ results in the production of IFN-γ

Received for publication March 25, 2004; accepted September 20, 2004.

From the *Department of Endoscopy, Hiroshima University Hospital, Hiroshima, Japan; the †Department of Medicine and Molecular Science, Hiroshima University, Hiroshima, Japan; the ‡Department of Immunology, National Institute of Neuroscience, NCNP, Tokyo, Japan; and the §Laboratory for Immune Regulation, RIKEN Research Center for Allergy and Immunology, and Department of Molecular Immunology, Graduate School of Medicine, Chiba University, Chiba, Japan.

This work was supported by grants from the Organization for Pharmaceutical Safety and Research.

Reprints: Shinji Tanaka, MD, PhD, Department of Endoscopy, Hiroshima University Hospital 1-2-3 Kasumi, Minami-ku, Hiroshima 734-8551, Japan (e-mail: colon@hiroshima-u.ac.jp).

only.[13,23,24] IL-12 stimulates NK1.1$^+$T cells to produce IFN-γ and inhibits their production of IL-4,[23,25,26] whereas IL-4 production by these cells requires IL-7 and is promoted by glucocorticoids.[27–29] Several costimulatory molecules play a role in the regulation of these cytokines. In the presence of blocking B7.2 (CD86) monoclonal antibody, αGalCer stimulation shifts the cytokine profile of NKT cells toward T helper (T_H) type 2 cells, whereas the presentation of αGalCer by CD40-activated antigen presenting cells causes a T_H1 shift of NKT cells.[30] Recently, Miyamoto et al[31] demonstrated that OCH, which has shorter hydrophobic chains than αGalCer, induces the production of, predominantly, IL-4 by NKT cells from murine spleen, leading to T_H2 bias in a Vα14 NKT cell-dependent manner. Therefore, the specific stimulation of NKT cells may have a therapeutic effect on various diseases associated with the T_H1-type or T_H2-type immune response.

The role of NKT cells in intestinal inflammation has been elucidated by several investigators. The ligand-specific activation of Vα14 NKT cells by αGalCer has been shown to protect mice against experimental colitis.[32] This protection was absent in CD1d$^{-/-}$ mice, and the elimination of NK1.1$^+$ cells reduced the effect of αGalCer. Other authors have reported that oxazolone-induced colitis, a T_H2-type colitis, is mediated by IL-13–producing NKT cells.[33] These results suggest that a CD1d–NKT cell interaction may be involved in the pathogenesis of colonic inflammation. However, the precise mechanism by which activated NKT cells modulate the pathogenesis of colitis is not yet understood. In the present study, we examined the role of NKT cells activated by OCH or αGalCer in protection against dextran sulfate sodium (DSS)-induced colitis. Our results indicate that the activation of Vα14 NKT cells by OCH shifted toward T_H2-type immune balance in the intestinal mucosa and that this is critical for protection against DSS-induced colitis.

MATERIALS AND METHODS

Mice

Specific pathogen-free C57BL/6 (B6) mice were purchased from Japan Clea (Tokyo, Japan). Jα281-deficient (Vα14 NKT cell-deficient [KO]) mice on a B6 background were generated, as described previously.[20] All mice were housed under specific pathogen-free conditions in microisolator cages in the animal facility at Hiroshima University, and only male mice (9 to 11 wk of age) were used.

DSS Colitis Model

DSS ([molecular weight, 5000] Wako Chemical Co, Osaka, Japan) was added to the water supply of the animals at a concentration of 1.5% (wt/vol) for days 1–9. The progression of colitis was monitored by a daily examination for rectal bleeding, perianal soiling, lack of grooming, hunched posture, weight loss, and mortality. Total body weight (in grams) was measured at the same time each day. All experiments were repeated at least twice with 5 to 15 mice.

In Vivo Injection of Glycolipid

OCH and αGalCer were first dissolved in dimethylsulfoxide at 100 μg/mL and then were diluted in phosphate-buffered saline (PBS) solution. To investigate the role of invariant NKT cells on the induction phase of DSS-induced colitis, each glycolipid (100 μg/kg in 200 μL of solution) was injected intraperitoneally on day 3 after the induction of colitis. Day 3 was selected because, in our preliminary studies, a single dose of glycolipids before the administration of DSS did not show any protective effect against DSS-induced colitis. Control animals received 200 μL of PBS solution containing the same concentration of dimethylsulfoxide (10%).

Assessment of the Severity of Colitis

Mice were killed on day 9 after DSS administration. Intestinal tissues were removed and opened longitudinally. The length of the colon was measured after the exclusion of the cecum and prior to division for histology. The tissues then were rolled concentrically and embedded in paraffin. Sections were stained with hematoxylin-eosin. The degree of inflammation of the colon was graded for severity according to mucosal damage (D) and the extension of the lesion (E) based on the method of Kitajima et al.[34] The histologic index was calculated as D plus E and was expressed as the mean of the score for each segment (i.e., for the cecum and the proximal, middle, and distal colon). The total score was the sum of the scores obtained in these sections. All slides were scored blindly.

Isolation of Colonic Lamina Propria Lymphocytes

Colonic lamina propria lymphocytes (LPLs) were isolated as described previously.[35] Briefly, nonadherent mesenteric tissues were removed, and the entire length of the intestine was opened longitudinally, washed with PBS solution, and cut into small (~5-mm) pieces. The dissected mucosa was incubated with $Ca^{++}Mg^{++}$-free Hanks balanced salt solution containing 1 mM ethylenediaminetetraacetic acid (Sigma, St. Louis, MO) for 20 minutes. Specimens were washed with Hanks balanced salt solution and then were incubated in 150 U/mL collagenase (Wako Chemical Co) in RPMI 1640 medium for 1.5 hours at 37 °C with stirring. Cells were suspended in 44% isotonic Percoll (Sigma) underlaid with 66% isotonic Percoll and were centrifuged for 20 minutes at 2200 revolutions per minute at room temperature. Cells at the interface were collected and washed twice with cold PBS. Approximately 2×10^6 cells per colon were recovered with >95% viability, as determined by trypan blue exclusion. Cells not excluding trypan blue were not included in the final count.

Cytokine Analysis in the Colonic Mucosa

Colonic LPLs were purified, transferred to 96-well plates (5×10^5 cells per well), and cultured for 48 hours in medium containing 500 ng/mL phorbol myristate acetate (PMA) (Sigma) and 50 ng/mL ionomycin (Sigma). After 48 hours, supernatants were harvested and stored at –20 °C until further analysis. The colon organ culture analysis for cytokines was performed as described previously.[36] Briefly, the mice were killed, the colon was removed, cut open longitudinally, and washed in PBS solution. The colonic tissue was transferred to 24-well flat-bottom culture plates containing fresh RPMI 1640 medium supplemented with penicillin and streptomycin, and was incubated at 37 °C for 24 hours. Culture supernatants were harvested and assayed for cytokines. IFN-γ, IL-4, and IL-10 were measured with OptEIA kits (BD, San Jose, CA). All samples were analyzed in triplicate.

Statistical Analysis

Data were analyzed with the Japanese version of StatView software (Hulinks, Tokyo, Japan) on a Macintosh Computer (Apple Computer, Cupertino, CA). The data are expressed as the mean ± SD. Differences between groups were examined for statistical significance with the Student *t* test after analysis of variance. Differences were considered to be statistically significant at $P < 0.05$.

RESULTS

Efficacy of In Vivo Glycolipid Treatment in DSS-Induced Colitis

As reported previously, OCH, a relatively new synthetic analogue of αGalCer, induces the production of IL-4 by NKT cells from murine spleen, leading to T_H2 bias in a Vα14 NKT cell-dependent manner.[31] To investigate whether the specific activation of Vα14 NKT cells by OCH protects against colitis, a single dose of OCH was administered to C57BL/6 mice by intraperitoneal injection on day 3 during the induction of colitis. As shown in Figure 1A, OCH-treated mice lost significantly less weight compared with PBS-treated mice. Gross rectal bleeding was seen in 60% of PBS-treated mice (6/10 mice) and in 10% of OCH-treated mice (1/10 mice) on day 9. OCH significantly prevented shortening of the colon (Fig. 1B). Histologic analysis confirmed the presence of marked inflammatory cell infiltrations with a loss of the mucosal surface in the colons of mice injected with PBS (Figs. 2A, D). In contrast, mononuclear cell infiltration was observed, but colonic crypts were still conserved in the colons of OCH-treated mice (Figs. 2B, E). The histologic scores of the severity of colitis were significantly reduced in the OCH-treated group (Figs. 3A, B). PBS-treated and OCH-treated mice began to lose their initial body weight on day 6 and day 8, respectively (Fig. 1A), and all OCH-treated animals had histologic colitis on day 9. OCH may therefore delay colitis by 2 days rather than provide complete protection from colitis.

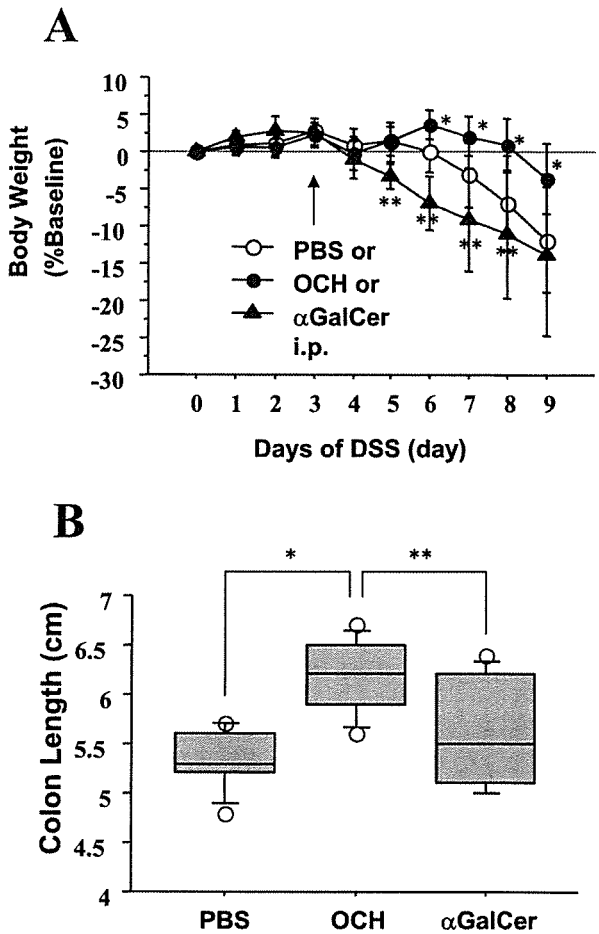

FIGURE 1. The effect of OCH on the protective immunity against DSS-induced colitis. A, C57BL/6 mice (n = 10 per group) were exposed continuously to 1.5% DSS in drinking water from day 0 to day 9. Mice were injected intraperitoneally with 100 μg/kg OCH, αGalCer, or PBS solution on day 3. Body weights of individual mice were recorded daily. The measurement of body weight, as a percentage of starting weight, is shown. * = $P < 0.005$ compared with mice treated with PBS; ** = $P < 0.05$ compared with mice treated with PBS. B, Comparison of colon lengths in DSS-treated mice on day 9. Each box plot represents 10 mice. * = $P < 0.0001$ for a comparison of OCH versus PBS; ** = $P < 0.05$ for a comparison of OCH versus αGalCer.

A single dose of αGalCer also improved the histologic score in the middle and proximal parts of the colon at the same levels as OCH treatment (Figs. 2 and 3A). When the scores were pooled with differences in the other sites, OCH was superior to αGalCer in histology (Fig. 3B). Gross rectal bleeding was observed in 50% of αGalCer-treated mice (5/10 mice) on day 9. In total, αGalCer treatment resulted in no differences in body weight changes, colon length, or total histologic scores in comparison with PBS treatment (Figs. 1–3). These data demonstrated that OCH is more effective in preventing DSS-

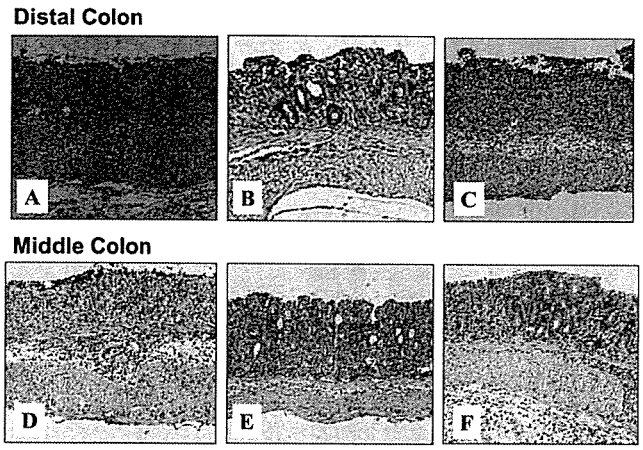

FIGURE 2. Histopathology of the colons from DSS-treated C57BL/6 mice. Representative photomicrographs (200×) of paraffin-embedded, hematoxylin-eosin–stained longitudinal sections of the distal parts of the colon (A–C) and the middle parts of the colon (D–F) from mice injected intraperitoneally with PBS solution (A and D), OCH (B and E), and αGalCer (C and F).

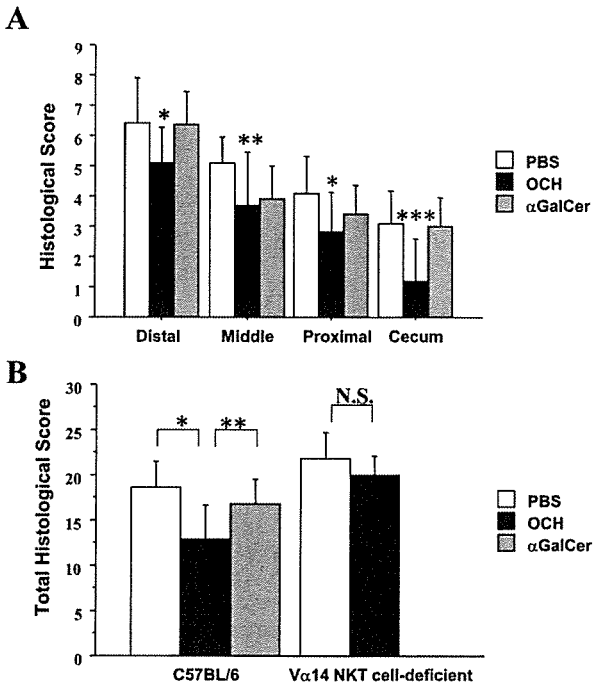

FIGURE 3. Histologic scores. Scoring was performed as described in "Materials and Methods." A, Histologic scores of each part of the colons. * = $P < 0.05$ for a comparison of PBS versus OCH; ** = $P < 0.05$ for a comparison of PBS versus OCH or αGalCer; and *** = $P < 0.005$ for a comparison of PBS versus OCH. B, Total histologic scores were expressed as the sum of the scores obtained in these sections. Vα14 NKT cell-deficient mice (n = 10 per group) also were treated with 1.5% DSS in drinking water from day 0 to day 9. The mice were injected intraperitoneally with 100 μg/kg OCH or PBS solution on day 3. * = $P < 0.005$ for a comparison of PBS versus OCH; ** = $P < 0.05$ for a comparison of OCH versus αGalCer in C57BL/6 mice; N.S. = not significant.

induced colitis than αGalCer. To confirm whether this protective effect of OCH was Vα14 NKT cell-dependent, we administered OCH to Vα14 NKT cell-deficient mice on day 3 during the induction of colitis. As shown in Figure 3B, OCH treatment had no effect on prevention of the development of DSS-induced intestinal inflammation in Vα14 NKT cell-deficient mice, as determined by evaluation of the total histologic score. These data indicated that the activation of Vα14 NKT cells by specific glycolipids influences protective immunity against intestinal inflammation.

Effect of Glycolipids on Mucosal Cytokine Balance

To examine whether the specific activation of Vα14 NKT cells by in vivo glycolipids could regulate the mucosal T_H1/T_H2 balance, we measured IFN-γ and IL-4 levels in supernatants from in vitro-stimulated colonic LPLs by enzyme-linked immunosorbent assay (ELISA) after the intraperitoneal injection of glycolipids. Colonic LPLs from DSS-treated C57BL/6 mice on days 5 and 9 produced significantly higher levels of both IFN-γ and IL-4 in comparison with those from non–DSS-treated, control, day 0 animals (Fig. 4A). The IFN-γ/IL-4 ratio increased in a time-dependent manner, suggesting that the progression of intestinal inflammation may be associated with T_H1-predominant immune responses (Fig. 4B). We next studied whether this ratio was affected by the administration of glycolipids. Treatment with both glycolipids induced higher amounts of IFN-γ and IL-4 than did PBS treatment (Fig. 4C, upper panels). When the IFN-γ/IL-4 ratio was calculated in each supernatant, both glycolipids significantly improved the ratio, and the degree of improvement by OCH was greater than that by αGalCer (Fig. 4C, lower panel). IL-10 had an anti-inflammatory effect on DSS-induced colitis.[37] We then analyzed IL-10 levels in the supernatants of colon organ cultures at an early phase after the injection of the glycolipids. Interestingly, OCH injection induced significantly higher IL-10 production than did αGalCer in the local colonic mucosa at 6 and 12 hours after injection (Figs. 5A, B). This IL-10 production was abrogated in Vα14 NKT cell-deficient mice, suggesting that the colonic mucosal IL-10 production is Vα14 NKT cell-dependent (data not shown). These data indicate that OCH induces a sufficient production of IL-10 in the local colonic mucosa and improves the subsequent mucosal T_H1/T_H2 cytokine balance at the time of development of colitis.

DISCUSSION

Here, we have shown that the specific activation of Vα14 NKT cells by OCH protects against DSS-induced colitis

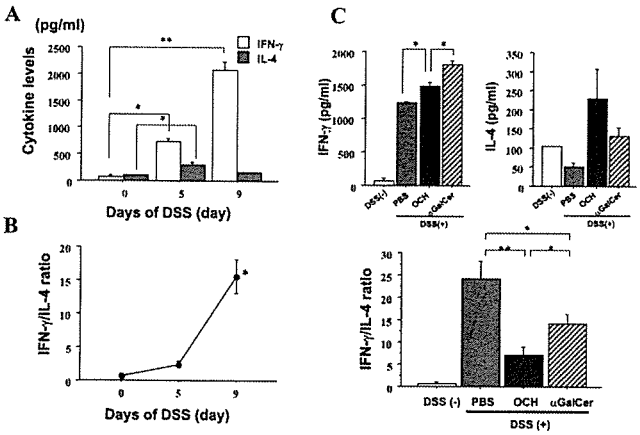

FIGURE 4. Comparison of the effects of glycolipids on mucosal cytokine balance in in vitro-stimulated colonic LPLs. A, C57BL/6 mice (n = 5 per group) were killed on the indicated days after 1.5% DSS administration, and colonic LPLs were purified. LPLs were stimulated in vitro with 500 ng/mL PMA and 50 ng/mL ionomycin, and were incubated at 37 °C for 48 hours. Supernatants were harvested, and cytokine levels were assessed by enzyme-linked immunosorbent assay. * = $P < 0.05$ for a comparison of day 0 versus day 5; ** = $P < 0.005$ for a comparison of day 0 versus day 9. B, Levels of IFN-γ and IL-4 were determined, and the IFN-γ/IL-4 ratio was calculated. * = $P < 0.005$ versus day 0. C, C57BL/6 mice treated with 1.5% DSS were injected with 100 μg/kg OCH, αGalCer, or PBS solution on day 3. The mice were killed on day 9, and colonic LPLs were purified. The LPLs were stimulated in vitro with 500 ng/mL PMA and 50 ng/mL ionomycin, and were incubated at 37 °C for 48 hours. Supernatants were harvested, and cytokine levels were analyzed by enzyme-linked immunosorbent assay. The amounts of IFN-γ and IL-4 were determined, and the IFN-γ/IL-4 ratio was calculated. DSS (−) and DSS (+) represent non-DSS-treated and DSS-treated mice, respectively. * = $P < 0.05$ for a comparison of OCH versus PBS or αGalCer, or PBS versus αGalCer. ** = $P < 0.01$ for a comparison of OCH versus PBS. Bars indicate the mean ± SD of 5 mice per group. The data are representative of 3 independent experiments.

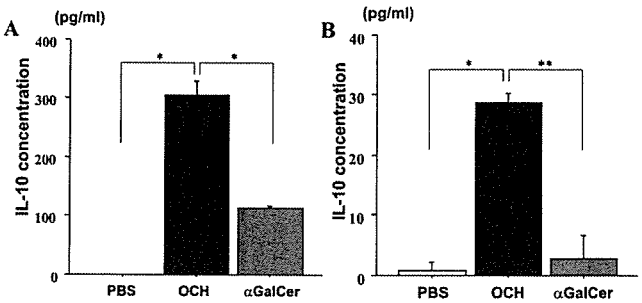

FIGURE 5. Rapid IL-10 induction after in vivo glycolipid injection during DSS administration. C57BL/6 mice treated with 1.5% DSS were injected with 100 μg/kg OCH, αGalCer, or PBS solution on day 3. The mice were killed 6 hours after injection (A) and 12 hours after injection (B), the colons were harvested, and organ culture was performed for cytokine analysis. The data are representative of 2 independent experiments. Bars indicate the mean ± SD of 5 mice per group. * = $P < 0.005$ for a comparison of OCH versus PBS or αGalCer; ** = $P < 0.05$ for a comparison of OCH versus αGalCer.

through the modulation of the mucosal T_H1/T_H2 cytokine balance.

It was recently reported that an analog of αGalCer, OCH, which has a truncated sphingosine chain, stimulates NKT cells to produce IL-4.[31] Therefore, OCH has the potential to elicit protective immunity against T_H1-mediated inflammatory disease. We have shown that a single dose of OCH attenuates DSS-induced colitis. This protection was mediated by Vα14 NKT cells because OCH did not elicit any protective effect in Vα14 NKT cell-deficient mice. In our preliminary study, we compared Vα14 NKT cell-deficient mice to wild-type B6 mice by administering 1.5% DSS. Interestingly, the knockout mice showed more severe intestinal inflammation when treated with DSS (our unpublished data). The loss of the protective effect of OCH in Vα14 NKT cell-deficient mice, however, may not be due to the increased susceptibility to DSS colitis because the effect of OCH was not observed when the knockout mice were given a lower dose (1.0%) of DSS (data not shown). These findings suggest that the specific activation of Vα14 NKT cells could reduce intestinal inflammation.

In contrast, a single dose of αGalCer, which was originally discovered as a ligand for NKT cells, had a smaller effect on prevention against DSS-induced colitis than OCH. Why do these glycolipids differ in the ability to protect against intestinal inflammation?

To examine the effects of these glycolipids on local immunologic responses, the levels of cytokines produced by colonic LPLs were analyzed. Colonic LPLs from DSS-treated C57BL/6 mice produced a significantly higher IFN-γ/IL-4 ratio in comparison to that from non–DSS-treated control animals. This ratio increased in a time-dependent fashion. We found in the present study that this ratio was significantly decreased by treatment with glycolipids, and OCH improved the ratio more significantly than αGalCer. The severity of the disease inversely correlated with the IFN-γ/IL-4 ratio. Therefore, OCH may prevent colitis through improvement of the mucosal T_H1/T_H2 cytokine balance.

The T_H1/T_H2 response in DSS-induced colitis remains unclear. It has been reported that DSS-induced colitis in C57BL/6 mice is characterized by a T_H1-type response with a strong induction of IFN-γ messenger RNA expression.[38] In DSS-treated mice, anti–IFN-γ and/or anti-tumor necrosis factor-α antibodies significantly reduce the severity of colitis.[39] On the other hand, the role of IL-4 in DSS-induced colitis is not fully understood. Stevceva et al[40] showed that DSS-induced colitis is ameliorated in IL-4–deficient mice, suggesting that even IL-4 may play a pathologic role in the intestinal inflammation induced by DSS. Therefore, the beneficial effects of the

glycolipids in the DSS-induced colitis model may not be due simply to an increase in IL-4 production.

Another T_H2-related cytokine, IL-10, has been widely characterized as an immunosuppressive cytokine and is important for mucosal immunologic homeostasis.[41–43] We also detected that OCH rapidly induces the localized expression of IL-10 in the colonic mucosa. How does OCH induce secretion of IL-10? Although we could not determine which cells in the colonic mucosa produce IL-10 in response to the activation of NKT cells by OCH, dendritic cells are one of the main producers of IL-10,[44] and CD1d-restricted NKT cells are known to contribute to immune function by regulating dendritic cell maturation.[45] A recent study showed that αGalCer stimulates the production of IL-12 by dendritic cells.[46] OCH has shorter hydrophobic chains than does αGalCer but has the same hydrophilic cap.[31] Therefore, OCH may bind to the CD1d groove less stably and may induce a weaker T-cell receptor signal to CD1d-restricted T cells than does αGalCer. Such T cells could induce antiinflammatory mature dendritic cells that produce more IL-10 than IL-12.[47] We hypothesized that the difference in the affinities of the glycolipids for the CD1d groove may influence the development of mature dendritic cells that preferentially produce IL-12 or IL-10. Since the murine colonic mucosa contains dendritic cells, which have a capacity to produce both IL-10 and IL-12,[48] it would be important to know whether these dendritic cell-derived cytokine balances are affected by activating NKT cells with glycolipids. Further studies are needed to clarify the precise mechanism underlying the protective immunity induced when NKT cells are activated.

It was recently shown that a course of multiple injections of αGalCer provides some protection against DSS-induced colitis.[32] Our present findings indicated that a single injection of αGalCer is not sufficient to elicit a preventive effect against DSS-induced colitis. This difference may be explained by the fact that single and multiple injections of αGalCer are known to induce specifically T_H1-predominant[49,50] and T_H2-predominant[51–53] immune responses, respectively. Miyamoto et al[31] reported that a single injection of OCH, but not of αGalCer, improves experimental allergic encephalomyelitis, a T_H1-associated disease, in mice. These previous findings and the results of the present study suggest that shifting toward a T_H2-type mucosal immune response may be crucial for protecting against DSS-induced colitis.

Heller et al[33] showed that oxazolone-induced colitis, a T_H2 colitis model, is mediated by IL-13–producing NKT cells. Whether NKT cells act as effector cells or regulatory cells may depend on the pathophysiology of the disease. Recently, Fuss et al[54] demonstrated the presence of IL-13–producing nonclassical NKT cells in the colonic mucosa of patients with ulcerative colitis. It would be interesting to examine the interaction between these pathogenic noninvariant mucosal NKT cells and anti-inflammatory invariant NKT cells. According to our present study, OCH may have potential as a treatment of human T_H1-predominant intestinal inflammatory diseases, such as Crohn's disease.[55]

In summary, we showed that Vα14 NKT cells are important for attenuating DSS-induced colitis. This protective immunity may be modulated by the activation status of Vα14 NKT cells. Although additional experiments are needed, our data indicate that an early and sufficient T_H2-biased immune response in the intestinal mucosa during the onset of colitis may have an antiinflammatory effect. Future studies with Vα14 NKT cell-deficient mice and analyses of the effects of glycolipids in other animal models of colitis will clarify our understanding of the pathologic process underlying colitis and will improve the chances of developing effective treatments for human inflammatory bowel disease.

REFERENCES

1. Taniguchi M, Harada M, Kojo S, et al. The regulatory role of Vα14 NKT cells in innate and acquired immune response. *Annu Rev Immunol.* 2003; 21:483–513.
2. Wilson SB, Delovitch TL. Janus-like role of regulatory iNKT cells in autoimmune disease and tumor immunity. *Nat Rev Immunol.* 2003;3:211–222.
3. Chan WL, Pejnovic N, Liew TV, et al. NKT cell subsets in infection and inflammation. *Immunol Lett.* 2003;85:159–163.
4. Wilson MT, Van Kaer L. Natural killer T cells as targets for therapeutic intervention in autoimmune diseases. *Curr Pharm Des.* 2003;9:201–220.
5. Lisbonne M, Leite-de-Moraes MC. Invariant Vα14 NKT lymphocytes: a double-edged immuno-regulatory T cell population. *Eur Cytokine Netw.* 2003;14:4–14.
6. Park SH, Roark JH, Bendelac A. Tissue-specific recognition of mouse CD1 molecules. *J Immunol.* 1998;160:3128–3134.
7. Mandal M, Chen XR, Alegre ML, et al. Tissue distribution, regulation and intracellular localization of murine CD1 molecules. *Mol Immunol.* 1998; 35:525–536.
8. Blumberg RS, van de Wal Y, Claypool S, et al. The multiple roles of major histocompatibility complex class-I-like molecules in mucosal immune function. *Acta Odontol Scand.* 2001;59:139–144.
9. Kaser A, Nieuwenhuis EE, Strober W, et al. CD1d-restricted T cell pathways at the epithelial-lymphocyte-luminal interface. *J Pediatr Gastroenterol Nutr.* 2004;39:S719–S722.
10. Kinebuchi M, Matsuura A. Rat T-cell receptor TRAV11 (Vα14) genes: further evidence of extensive multiplicity with homogeneous CDR1 and diversified CDR2 by genomic contig and cDNA analysis. *Immunogenetics.* 2004;55:756–762.
11. Natori T, Koezuka Y, Higa T. Agelasphins, novel α-galactosylceramides from marine sponge *Agelas mauritianus. Tetrahedron Lett.* 1993;34: 5591–5592.
12. Natori T, Morita M, Akimoto K, et al. Agelasphins, novel antitumor and immunostimulatory cerebrosides from marine sponge *Agelas mauritianus. Tetrahedron.* 1994;50:2771–2784.
13. Kawano T, Cui J, Koezuka Y, et al. CD1d-restricted and TCR-mediated activation of V alpha 14 NKT cells by glycosylceramides. *Science.* 1997; 278:1626–1629.
14. Burdin N, Brossay L, Koezuka Y, et al. Selective ability of mouse CD1 to present glycolipids: α-galactosylceramide specifically stimulates $V\alpha14^+$ NKT lymphocytes. *J Immunol.* 1998;161:3271–3281.
15. Gombert JM, Herbelin A, Tancrede-Bohin E, et al. Early quantitative and functional deficiency of $NK1^+$-like thymocytes in the NOD mouse. *Eur J Immunol.* 1996;26:2989–2998.
16. Hammond KJ, Poulton LD, Palmisano LJ, et al. α/β-T cell receptor $(TCR)^+CD4^-CD8^-$(NKT) thymocytes prevent insulin-dependent diabetes mellitus in nonobese diabetic (NOD)/Lt mice by the influence of interleukin (IL)-4 and/or IL-10. *J Exp Med.* 1998;187:1047–1056.
17. Mieza MA, Itoh T, Cui JQ, et al. Selective reduction of $V\alpha14^+$ NKT cells

associated with disease development in autoimmune-prone mice. *J Immunol.* 1996;156:4035–4040.
18. Wilson SB, Kent SC, Patton KT, et al. Extreme Th1 bias of invariant Vα24JαQ T cells in type-I diabetes. *Nature.* 1998;391:177–181.
19. Cui J, Shin T, Kawano T, et al. Requirement for Vα14 NKT cells in IL-12-mediated rejection of tumors. *Science.* 1997;278:1623–1626.
20. Kawano T, Cui J, Koezuka Y, et al. Natural killer-like nonspecific tumor cell lysis mediated by specific ligand-activated Vα14 NKT cells. *Proc Natl Acad Sci USA.* 1998;95:5690–5693.
21. Takeda K, Seki S, Ogasawara K, et al. Liver NK1.1$^+$CD4$^+$αβ T cells activated by IL-12 as a major effector in inhibition of experimental tumor metastasis. *J Immunol.* 1996;156:3366–3373.
22. Toura I, Kawano T, Akutsu Y, et al. Inhibition of experimental tumor metastasis by dendritic cells pulsed with α-galactosylceramide. *J Immunol.* 1999;163:2387–2391.
23. Arase H, Arase N, Saito T. Interferon γ production by natural killer (NK) cells and NK1.1$^+$T cells upon NKR-P1 cross-linking. *J Exp Med.* 1996; 183:2391–2396.
24. Chen H, Paul WE. Cultured NK1.1$^+$CD4$^+$T cells produce large amounts of IL-4 and IFN-γ upon activation by anti-CD3 or CD1. *J Immunol.* 1997; 159:2240–2249.
25. Emoto M, Emoto Y, Kaufmann SH. Bacille Calmette Guerin and interleukin-12 down-modulate interleukin-4 producing CD4$^+$NK1$^+$T lymphocytes. *Eur J Immunol.* 1997;27:183–188.
26. Leite-De-Moraes MC, Moreau G, Arnould A, et al. IL-4 producing NK T cells are biased towards IFN-γ production by IL-12. Influence of the microenvironment on the functional capacities of NKT cells. *Eur J Immunol.* 1998;28:1507–1515.
27. Vicari AP, Herbelin A, Leite-De-Moraes MC, et al. NK1.1$^+$T cells from interleukin-7 deficient mice have a normal distribution and selection but exhibit impaired cytokine productioin. *Int Immunol.* 1996;8:1759–1766.
28. Leite-De-Moraes MC, Herbelin A, Gombert JM, et al. Requirement of IL-7 for IL-4-producing potential of MHC class I-selected CD4$^-$CD8$^-$TCRαβ$^+$thymocytes. *Int Immunol.* 1997;9:73–79.
29. Tamada K, Harada M, Abe K, et al. IL-4-producing NK1.1$^+$T cells are resistant to glucocorticoid-induced apoptosis: implications for the Th1/Th2 balance. *J Immunol.* 1998;161:1239–1247.
30. Pal E, Tabira T, Kawano T, et al. Costimulation-dependent modulation of experimental autoimmune encephalomyelitis by ligand stimulation of Vα14 NKT cells. *J Immunol.* 2001;166:662–668.
31. Miyamoto K, Miyake S, Yamamura T. A Synthetic glicolipid prevents autoimmune encephalomyelitis by inducing T_H2 bias of natural killer T cells. *Nature.* 2001;413:531–534.
32. Saubermann LJ, Beck P, De Jong YP, et al. Activation of natural killer T cells by α-galactosylceramide in the presence of CD1d provides protection against colitis in mice. *Gastroenterology.* 2000;119:119–128.
33. Heller F, Fuss IJ, Nieuwenhuis EE, et al. Oxazolone colitis, a Th2 colitis model resembling ulcerative colitis, is mediated by IL-13-producing NK-T cells. *Immunity.* 2002;17:629–638.
34. Kitajima S, Takuma S, Morimoto M. Histological analysis of murine colitis induced by dextran sulfate sodium of different molecular weights. *Exp Anim.* 2000;49:9–15.
35. Okamoto S, Watanabe M, Yamazaki M, et al. A synthetic mimetic CD4 is able to suppress disease in a rodent model of immune colitis. *Eur J Immunol.* 1999;29:355–366.
36. Siegmund B, Lehr HA, Fantuzzi G, *et al.* 2001. IL-1β-converting enzyme (caspase-1) in intestinal inflammation. *Proc Natl Acad Sci USA.* 2001;98: 13249–13254.
37. De Winter H, Elewaut D, Turovskaya O, et al. Regulation of mucosal immune responses by recombinant interleukin 10 produced by intestinal epithelial cells in mice. *Gastroenterology.* 2002;122:1829–1841.
38. Andres PG, Beck PL, Mizoguchi E, et al. Mice with a selective deletion of the CC chemokine receptors 5 or 2 are protected from dextran sodium sulfate-mediated colitis:lack of CC chemokine receptor 5 expression results in a NK1.1$^+$ lymphocyte-associated Th2-type immune response in the intestine. *J Immunol.* 2000;164:6303–6312.
39. Obermeier F, Kojouharoff G, Hans W, et al. Interferon-γ and tumor necrosis factor-induced nitric oxide as toxic effector molecule in chronic dextran sulfate sodium-induced colitis in mice. *Clin Exp Immunol.* 1999; 116:238–245.
40. Stevceva L, Pavli P, Husband A, et al. Dextran sulphate sodium-induced colitis is ameliorated in interleukin 4 deficient mice. *Genes Immun.* 2001; 2:309–316.
41. Steidler L, Hans W, Schotte L, et al. Treatment of murine colitis by *Lactococcus lactis* secreting interleukin-10. *Science.* 2000;289:1352–1355.
42. Mizoguchi A, Mizoguchi E, Takedatsu H, et al. Chronic intestinal inflammatory condition generates IL-10-producing regulatory B cell subset characterized by CD1d upregulation. *Immunity.* 2002;16:219–230.
43. Colgan SP, Hershberg RM, Furuta GT, et al. Ligation of intestinal epithelial CD1d induces bioactive IL-10: critical role of the cytoplasmic tail in autocrine signaling. *Proc Natl Acad Sci USA.* 1999;96:13938–13943.
44. Lutz MB, Schuler G. Immature, semi-mature and fully mature dendritic cells: which signals induce tolerance or immunity? *Trends Immunol.* 2002;23:445–449.
45. Vincent MS, Leslie DS, Gumperz JE, et al. CD1-dependent dendritic cell instruction. *Nat Immunol.* 2002;3:1163–1168.
46. Kitamura H, Iwakabe K, Yahata T, et al. The natural killer T (NKT) cell ligand α-galactosylceramide demonstrates its immunopotentiating effect by inducing interleukin (IL)-12 production by dendritic cells and IL-12 receptor expression on NKT cells. *J Exp Med.* 1999;189:1121–1128.
47. Vincent MS, Gumperz JE, Brenner MB. Understanding the function of CD1-restricted T cells. *Nat Immunol.* 2003;4:517–523.
48. Krajina T, Leithauser F, Moller P, et al. Colonic lamina propria dendritic cells in mice with CD4$^+$ T cell-induced colitis. *Eur J Immunol.* 2003;33: 1073–1083.
49. Kawakami K, Kinjo Y, Yara S, et al. Activation of Vα14$^+$ natural killer T cells by α-galactosylceramide results in development of Th1 response and local host resistance in mice infected with *Cryptococcus neoformans. Infect Immun.* 2001;69:213–220.
50. Gonzalez-Aseguinolaza G, de Oliveira C, Tomaska M, et al. α-Galactosylceramide-activated Vα14 natural killer T cells mediate protection against murine malaria. *Proc Natl Acad Sci USA.* 2000;97:8461–8466.
51. Burdin N, Brossay L, Kronenberg M. Immunization with α-galactosylceramide polarizes CD1-reactive NK T cells towards Th2 cytokine synthesis. *Eur J Immunol.* 1999;29:2014–2025.
52. Hong S, Wilson MT, Serizawa I, et al. The natural killer T-cell ligand α-galactosylceramide prevents autoimmune diabetes in non-obese diabetic mice. *Nat Med.* 2001;7:1052–1056.
53. Sharif S, Arreaza GA, Zucker P, et al. Activation of natural killer T cells by α-galactosylceramide treatment prevents the onset and recurrence of autoimmune type I diabetes. *Nat Med.* 2001;7:1057–1062.
54. Fuss IJ, Heller F, Boirivant M, et al. Nonclassical CD1d-restricted NKT cells that produce IL-13 characterize an atypical Th2 response in ulcerative colitis. *J Clin Invest.* 2004;113:1490–1497.
55. Podolsky DK. Inflammatory bowel disease. *N Engl J Med.* 2002;347: 417–429.

JOC*Note*

Total Synthesis of an Immunosuppressive Glycolipid, (2*S*,3*S*,4*R*)-1-*O*-(α-D-Galactosyl)-2-tetracosanoylamino-1,3,4-nonanetriol

Kenji Murata,† Tetsuya Toba,† Kyoko Nakanishi,† Bitoku Takahashi,† Takashi Yamamura,‡ Sachiko Miyake,‡ and Hirokazu Annoura*,†

Daiichi Suntory Biomedical Research Co., Ltd., 1-1-1, Wakayamadai, Shimamoto-cho, Mishima-gun, Osaka 618-8513, Japan, and Department of Immunology, National Institute of Neuroscience, National Center for Neuroscience and Psychiatry, Tokyo 187-8502, Japan

hirokazu_annoura@dsup.co.jp

Received October 20, 2004

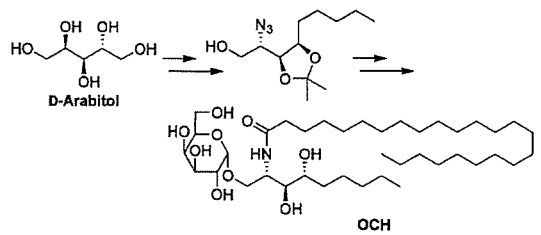

A practical and efficient total synthesis of (2*S*,3*S*,4*R*)-1-*O*-(α-D-galactosyl)-2-tetracosanoylamino-1,3,4-nonanetriol, OCH **1b**, a potential therapeutic candidate for Th1-mediated autoimmune diseases, is described. The synthesis incorporates direct alkylation onto epoxide **5** and stereospecific halide ion catalyzed α-glycosidation reaction. A key intermediate **10** was obtained in only eight steps and 37% overall yield from commercially available D-arabitol **2**, and the total synthesis of **1b** was accomplished in 12 steps and 19% overall yield. This method will enable the synthesis of a variety of phytosphingolipids, especially that with the shorter sphingosine side chain than **1a**, in a highly stereoselective manner.

Natural killer (NK) T cells are potent producers of immunoregulatory cytokines and specific for glycolipid antigens bound by a nonpolymorphic major histocompatibility complex (MHC) class I-like molecule, CD1d.[1] The glycolipids, an α-galactosylceramide named KRN7000 **1a**[2] and an altered analogue, OCH **1b**,[3] possessing a shorter C5 sphingosine side chain, have been identified as NKT cell ligands (Figure 1). Whereas **1a** has been shown to cause both interferon (IFN)-γ and interleukin

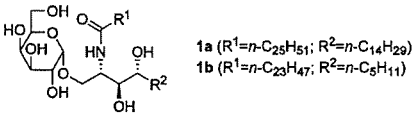

FIGURE 1. Structure of KRN7000 **1a** and OCH **1b**.

(IL)-4 production, **1b** induces a predominant production of IL-4, a key Th2 cytokine controlling autoimmunity. Compound **1b** is significantly effective in animal models of Th1-mediated autoimmune diseases such as experimental autoimmune encephalomyelitis (EAE) and collagen-induced arthritis (CIA), while **1a** showed only a minor effect.[3,4] It has recently been demonstrated that conversion of **1a** to its C-glycoside analogue leads to striking enhancement of activity on in vivo animal models of malaria and lung cancer.[5] Furthermore, similar substances including a tetraglycosylated glycolipid have recently been isolated from *Agelas Clathrodes*.[6] Consequently, considerable attention has been generated among synthetic chemists toward **1a**, **1b**, and their derivatives as new synthetic targets because of their distinctive biological and pharmacological properties as well as unique structural features. We present herein a practical and efficient total synthesis of immunosuppressive glycolipid **1b**.[7]

The significant structural difference between **1a** and **1b** is the length of a sphingosine side chain R^2. Reported procedures[2,8] for the syntheses of **1a** and its sphingosine derivatives, which essentially utilize Wittig-type or aldol-type reaction for the installation of the sphingosine side chain, gave low overall yields for **1b** and its analogues with a chain length shorter than C5 for R^2 and proved to be impractical.[9] Our strategy for resolving this problem is based upon the direct alkylation on epoxide **5**, which

* To whom correspondence should be addressed. Phone: +81-75-962-8188. Fax: +81-75-962-6448.
† Daiichi Suntory Biomedical Research Co., Ltd.
‡ National Institute of Neuroscience, NCNP.

(1) For reviews: (a) Porcelli, S. A.; Modlin, R. L. *Annu. Rev. Immunol.* **1999**, *17*, 297. (b) Hong, S.; Scherer, D. C.; Singh, N.; Mendiratta, S. K.; Serizawa, I.; Koezuka, Y.; Van Kaer, L. *Immunol. Rev.* **1999**, *169*, 31. (c) Sidobre, S.; Kronenberg, M. *J. Immunol. Methods* **2002**, *268*, 107. (d) Wilson, M. T.; Van Kaer, L. *Curr. Pharm. Des.* **2003**, *9*, 201. (e) Brigl, M.; Brenner, M. B. *Annu. Rev. Immunol.* **2004**, *22*, 817.

(2) (a) Morita, M.; Motoki, K.; Akimoto, K.; Natori, T.; Sakai, T.; Sawa, E.; Yamaji, K.; Koezuka, Y.; Kobayashi, E.; Fukushima, H. *J. Med. Chem.* **1995**, *38*, 2176. (b) Morita, M.; Sawa, E.; Yamaji, K.; Sakai, T.; Natori, T.; Koezuka, Y.; Fukushima, H.; Akimoto, K. *Biosci. Biotechnol. Biochem.* **1996**, *60*, 288. (c) Takikawa, H.; Muto, S.; Mori, K. *Tetrahedron* **1998**, *54*, 3141. (d) Graziani, A.; Passacantilli, P.; Piancatelli, G.; Tani, S. *Tetrahedron: Asymmetry* **2000**, *11*, 3921. (e) Plettenburg, O.; Bodmer-Narkevitch, V.; Wong C.-H. *J. Org. Chem.* **2002**, *67*, 4559.

(3) (a) Miyamoto, K.; Miyake, S.; Yamamura, T. *Nature* **2001**, *413*, 531. (b) Yamamura, T.; Miyake, S. PCT Int. Appl. WO 2003/016326, 2003; *Chem. Abstr.* **2003**, *138*, 205292m. (c) Yamamura, T.; Miyamoto, K.; Illes, Z.; Pal, E.; Araki, M.; Miyake, S. *Curr. Top. Med. Chem.* **2004**, *4*, 561. (d) Oki, S.; Chiba, A.; Yamamura, T.; Miyake, S. *J. Clin. Invest.* **2004**, *113*, 1631.

(4) Chiba, A.; Oki, S.; Miyamoto, K.; Hashimoto, H.; Yamamura, T.; Miyake, S. *Arthritis Rheum.* **2004**, *50*, 305.

(5) (a) Schmieg, J.; Yang, G.; Frank, R. W.; Tsuji, M. *J. Exp. Med.* **2003**, *198*, 1631. (b) Yang, G.; Schmieg, J.; Tsuji, M.; Frank, R. W. *Angew. Chem., Int. Ed.* **2004**, *43*, 3818.

(6) Costantino, V.; Fattorusso, E.; Imperatore, C.; Mangoni, A. *J. Org. Chem.* **2004**, *69*, 1174.

(7) Annoura, H.; Murata, K.; Yamamura, T. PCT Int. Appl. WO2004/072091, 2004; *Chem. Abstr.* **2004**, *141*, 225769n.

(8) (a) Schmidt, R. R., Maier, T. *Carbohydr. Res.* **1988**, *174*, 169. (b) Kobayashi, S.; Hayashi, T.; Kawasuji, T. *Tetrahedron Lett.* **1994**, *35*, 9573. (c) Azuma, H.; Tamagaki, S.; Ogino, K. *J. Org. Chem.* **2000**, *65*, 3538. (d) Fernandes, R. A.; Kumar, P. *Tetrahedron Lett.* **2000**, *41*, 10309. (e) Ndakala, J.; Hashemzadeh, M.; So, R. C.; Howell, A. R. *Org. Lett.* **2002**, *4*, 1719. (f) Ayad, T.; Génisson, Y.; Verdu, A.; Baltas, M.; Gorrichon, L. *Tetrahedron Lett.* **2003**, *44*, 579. (g) Lin, C.-C.; Fan, G.-T.; Fang, J.-M. *Tetrahedron Lett.* **2003**, *44*, 5281. (h) Chiu, H.-Yi; Tzou, D.-L. *J. Org. Chem.* **2003**, *68*, 5788.

10.1021/jo048151y CCC: $30.25
Published on Web 02/16/2005

SCHEME 1[a]

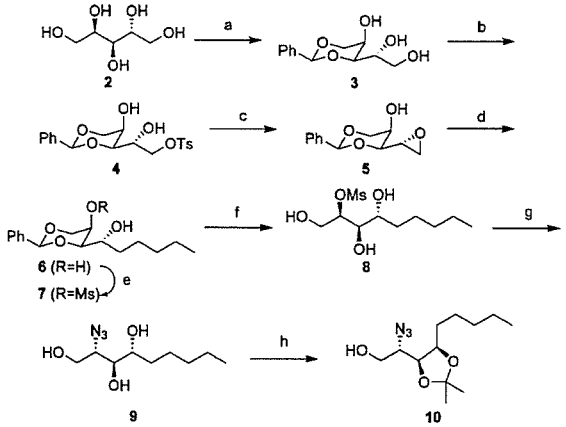

[a] Reagents and conditions: (a) PhCHO, dry HCl, rt, 91%; (b) *p*-TsCl, Et_3N, cat. Bu_2SnO, CH_2Cl_2, rt, quant; (c) *t*-BuOK, THF, rt, 91%; (d) *n*-Bu_2CuLi, THF, −40 °C, 98%; (e) MsCl, pyridine, −40 °C, 93%; (f) H_2, cat. $Pd(OH)_2$, EtOH, rt, quant; (g) NaN_3, DMF, 95 °C, 66%; (h) (i) cat. *p*-TsOH, 2,2-dimethoxypropane, rt; (ii) MeOH, rt, 75%.

has adequate stereocenters for the desired sphingosine side chain.[10]

Upon treatment of compound **3**,[11] which was readily prepared from D-arabitol **2** and benzaldehyde in 91% yield, with *p*-toluenesulfonyl chloride (*p*-TsCl) and triethylamine in the presence of a catalytic amount of dibutyltin oxide (Bu_2SnO),[12] regiospecific tosylation proceeded at the primary alcohol moiety to give **4** quantitatively (Scheme 1). The use of Bu_2SnO not only reduced the cost of this transformation but also greatly simplified the purification process since the yield was decreased to less than 30% when the reaction was carried out in the absence of Bu_2SnO. Treatment of **4** with *t*-BuOK produced the requisite epoxide **5** in 91% yield. Direct *n*-butylation onto **5** using organocopper lithium reagent in THF at −40 to −20 °C afforded 1,3-*O*-benzylidene-1,2,3,4-nonanetetrol **6** in 98% yield as the single product. Regioselective mesylation of the axial-OH in **6** with 1 equiv of methanesulfonyl chloride (MsCl) in pyridine at −40 °C to room temperature afforded **7** in 93% yield.

SCHEME 2[a]

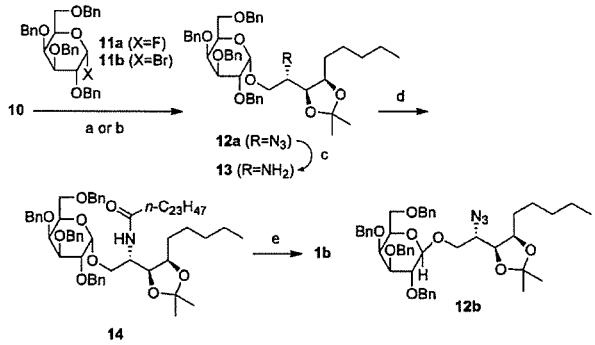

[a] Reagents and conditions: (a) **11a**, $BF_3{\cdot}Et_2O$, MS4Å, $CHCl_3$, −50 °C, 57% for **12a**, 25% for **12b**; (b) **11b**, *n*-Bu_4NBr, MS4Å, DMF−toluene (1:2.5), rt, 68% for **12a**; (c) H_2, Lindlar catalyst, EtOH, rt, quant; (d) *n*-$C_{23}H_{47}COOH$, EDCI, HOBt, *i*-Pr_2NEt, DMF−CH_2Cl_2 (1:3.5), 40 °C, 89%; (e) (i) HCl-dioxane, rt; (ii) H_2, cat. $Pd(OH)_2$, MeOH−$CHCl_3$ (3:1), rt, 84%

Deprotection of the benzylidene acetal in **7** by hydrogenation at atmospheric pressure in the presence of palladium hydroxide [$Pd(OH)_2$] in EtOH and subsequent azidation of **8** with sodium azide in DMF afforded **9** in 66% overall yield. Protection of the vicinal diols in **9** with a catalytic amount of *p*-toluenesulfonic acid (*p*-TsOH) in 2,2-dimethoxypropane at room temperature and quenching with MeOH afforded 3,4-isopropylidene acetal **10** in 75% yield.

As the key intermediate **10**, a glycosyl acceptor, was available, we next examined α-selective glycosidation reaction employing a variety of Lewis acids. After extensive experimentation, we found that glycosidation catalyzed by $BF_3{\cdot}Et_2O$ or *n*-Bu_4NBr with molecular sieves 4Å (MS4Å) worked well, but $AgClO_4$ reported for the synthesis[2] of **1a** gave only the undesired β-glycosylated product. Thus, treatment of **10** with benzyl protected galactosyl fluoride **11a** (1.8 equiv) in the presence of $BF_3{\cdot}Et_2O$ and MS4Å in $CHCl_3$ at −50 °C afforded α-galactosylceramide **12a** in 57% yield along with its β-isomer **12b** in 25% yield (Scheme 2). The stereochemistry of galactoside linkage was unambiguously determined by their NMR spectra[13] as well as conversion of **12a** into **1b** (vide infra). Surprisingly, when benzyl protected galactosyl bromide **11b**[14a] (1.8 equiv) and *n*-Bu_4NBr[14b] (3 equiv) with MS4Å were employed in toluene−DMF (2.5:1) at room temperature, **12a** was exclusively obtained in 68% yield. The corresponding β-galactosylated isomer **12b** could not be detected on TLC and NMR spectra. Upon using other ammonium bromides such as *n*-Hex_4NBr and Et_4NBr, the isolated yield of **12a** was decreased.

(9) According to the procedure reported in ref 2a, periodate oxidation of readily available tri-*O*-benzyl-D-galactose followed by Wittig-type reaction with a 5-fold molar excess of butylidene(triphenyl)phosphorane gave the desired (2*R*,3*S*,4*R*)-1,3,4-tri-*O*-benzyl-5-nonane-1,2,3,4-tetraol in less than 20% yield and consequently gave **1b** in low overall yield; see ref 3b. Also, when the more practical method for **1a** reported by Wong et al.[2e] was pursued for **1b**, similar Wittig reaction employing 3,4-di-*O*-benzyl-2-deoxy-6-*O*-triisopropylsilyl-D-galactopyranoside and propylidene(triphenyl)phosphorane resulted in complex mixtures containing an unavoidable byproduct in which the 3-benzyloxy group of galactopyranoside was eliminated. Therefore, our method is more efficient and practical for the synthesis of **1b** than those previously reported; however, this might not be the case for the synthesis of **1a**.

(10) During the preparation of this manuscript, Savage et al. have reported an alternative and efficient route for **1b**, although it requires the separation step of a 2:1 mixture of diastereomeric diols: Goff, R. D.; Gao, Y.; Mattner, J.; Zhou, D.; Yin, N.; Cantu, C., III; Teyton, L.; Bendelac, A.; Savage, P. B. *J. Am. Chem. Soc.* **2004**, *126*, 13602.

(11) (a) Hudson, C. S.; Hann, R. M.; Haskins, W. T. *J. Am. Chem. Soc.* **1943**, *65*, 1663. (b) Hough, L.; Theobald, R. S. *Methods Carbohydr. Chem.* **1963**, *1*, 94. (c) Dew, K. N.; Church, T. J.; Basu, B.; Vuorinen, T.; Serianni, A. S. *Carbohydr. Res.* **1996**, *284*, 135.

(12) Martinelli, M. J.; Nayyar, N. K.; Moher, E. D.; Dhokte, U. P.; Pawlak, J. M.; Vaidyanathan, R. *Org. Lett.* **1999**, *1*, 447.

(13) In the ^{13}C NMR (100 MHz, $CDCl_3$), the signal attributable to the anomeric carbon of **12a** appeared at δ 99.3, whereas that of **12b** was at δ 104.1. For ^{13}C NMR of glycosides: Pretsch, E.; Buhlmann, P.; Affolter, C. In *Structure Determination of Organic Compounds*, 3rd ed.; Springer-Verlag: 2000; pp 152−153. Also, in the ^1H NMR (400 MHz, $CDCl_3/CD_3OD$ 3:1) of **1b** derived from **12a**, the signal assignable to the hydrogen on the anomeric position was at δ 4.71 (d, 1H, J = 3.8 Hz), showing α-glycosidation product.

(14) Halide ion catalyzed glycosidation reaction was reported for the synthesis of α-linked disaccharide: (a) Spohr, U.; Le, N.; Ling, C.-C.; Lemieux, R. U. *Can. J. Chem.* **2001**, *79*, 238. (b) Lemieux, R. U.; Hendriks, K. B.; Stick, R. V.; James, K. *J. Am. Chem. Soc.* **1975**, *97*, 4056. Similar glycosidation methodology although in lower yield was reported: (c) Vo-Hoang, Y.; Micouin, L.; Ronet, C.; Gachelin, G.; Bonin, M. *ChemBioChem* **2003**, *4*, 27.

Selective reduction of the azido group of **12a** was achieved by hydrogenation with Lindlar catalyst in EtOH at room temperature to give amine **13** quantitatively. Compound **13** was acylated with *n*-tetracosanoic acid in the presence of 1-[3-(dimethylamino)propyl]-3-ethylcarbodiimide hydrochloride (EDCI), 1-hydroxybenzotriazole (HOBt) and *N,N*-diisopropylethylamine (*i*-Pr_2NEt) at 40 °C in DMF–CH_2Cl_2 (1:3.5) to afford amide **14** in 89% yield. Finally, deprotection of the isopropylidene acetal of **14** under acidic conditions and subsequent removal of the benzyl groups by hydrogenation with $Pd(OH)_2$ in MeOH–$CHCl_3$ (3:1) at room temperature furnished **1b** in 84% yield. The synthetic sample displayed satisfactory ^1H and ^{13}C NMR spectra, FABMS, and elemental analysis [mp 142–145 °C (recrystalized from EtOH/H_2O), $[\alpha]^{30}_D$ +53.9 (*c* 0.5, pyridine)].

In conclusion, we have developed an efficient and practical protocol for the synthesis of **1b** involving 12 steps starting from commercially available D-arabitol **2** in 19% overall yield. The key intermediate **10** as a glycosyl acceptor was obtained in only eight steps and 37% overall yield. Our method, amenable for large-scale synthesis, can provide a dozen grams of **1b** and enables the synthesis of a variety of phytosphingolipids related to **1a** and **1b**, especially those with the shorter sphingosine side chain or substituents other than aliphatic alkyl groups, in a highly stereoselective manner. The synthesis and structure–activity relationships of this series of compounds will be reported elsewhere in due course.[7]

Experimental Section

1,3-*O*-Benzylidene-D-arabitol (3). According to the reported procedures,[11] dry HCl was slowly bubbled into a mixture of D-arabitol **2** (98.8 g, 649 mmol) and benzaldehyde (78.8 mL, 775 mmol) for 15 min at room temperature. The mixture was allowed to stand at room temperature for 18 h. The resulting solid crystalline mass was broken up and placed in an evacuated desiccator containing KOH and H_2SO_4 for 24 h. The mass was triturated with Et_2O, neutralized with sat. $NaHCO_3$ aq., and filtered and washed with H_2O until the pH of the filtrate was neutral. The product was washed with Et_2O and recrystallized from 2-PrOH containing 0.5% v/v NH_4OH to give **3** (142.2 g, 91% yield) as colorless crystals; mp 130–131 °C; ^1H NMR (CD_3OD) δ 7.51–7.30 (m, 5H), 5.58 (*s*, 1H), 4.18 (d, 1H, J = 12 Hz), 4.11 (d, 1H, J = 12 Hz), 3.87–3.28 (m, 5H); HRMS calcd for $C_{12}H_{17}O_5$ $[M + H]^+$ 241.1076, found 241.1086.

1,3-*O*-Benzylidene-5-*O*-toluenesulfonyl-D-arabitol (4). To a suspension of **3** (34.0 g, 141 mmol) in CH_2Cl_2 (1200 mL) were added *p*-toluenesulfonyl chloride (27.0 g, 141 mmol), triethylamine (19.7 mL, 141 mmol) and dibutyltinoxide (702 mg, 2.82 mmol) at 0 °C. After being stirred for 21 h at room temperature, the mixture was concentrated in vacuo. The obtained residue was purified by column chromatography (CH_2Cl_2/MeOH 20:1) to give **4** (55.3 g, quant) as a white solid: ^1H NMR (DMSO-d_6) δ 7.73 (d, 2H, J = 8.2 Hz), 7.37–7.24 (m, 7H), 5.43 (s, 1H), 5.34 (d, 1H, J = 6.1 Hz), 4.77 (d, 1H, J = 6.5 Hz), 4.11 (dd, 1H, J = 9.8, 1.9 Hz), 4.04–3.85 (m, 4H), 3.71 (d, 1H, J = 9.2 Hz), 3.59 (d, 1H, J = 5.7 Hz), 2.32 (s, 3H); ^{13}C NMR ($CDCl_3$) δ 145.1, 137.3, 132.5, 129.9, 129.1, 128.2, 128.0, 125.8, 101.0, 77.9, 72.4, 70.9, 67.6, 62.7, 21.6; MS-ESI (*m/z*) 395 $[M + H]^+$; HRMS–FAB (*m/z*) $[M + H]^+$ calcd for $C_{19}H_{23}O_7S$, 395.1164, found 395.1189.

4,5-Anhydro-1,3-*O*-benzylidene-D-arabitol (5). To a solution of **4** (51.1 g, 130 mmol) in dry THF (800 mL) was added potassium *tert*-butoxide (18.1 g, 161 mmol) at 0 °C. The reaction mixture was stirred for 38 h at room temperature and then quenched with water. After being extracted with ethyl acetate, the organic layer was washed with brine, dried over anhydrous Na_2SO_4, and concentrated in vacuo. The residue was purified by column chromatography (*n*-hexane/EtOAc 1:1) to give **5** (26.2 g, 91%) as a white solid: ^1H NMR ($CDCl_3$) δ 7.52–7.34 (m, 5H), 5.57 (s, 1H), 4.25 (dd, 1H, J = 12, 1.8 Hz), 4.08 (dd, 1H, J = 12, 1.2 Hz), 3.78–3.75 (m, 2H), 3.35–3.31 (m, 1H), 2.93–2.84 (m, 3H); ^{13}C NMR ($CDCl_3$) δ 137.4, 129.3, 128.4, 126.0, 101.4, 79.7, 72.3, 64.4, 50.8, 45.9; MS-ESI (*m/z*) 223 $[M + H]^+$; HRMS–FAB (*m/z*) $[M + H]^+$ calcd for $C_{12}H_{15}O_4$, 223.0971, found 223.0895.

(2*R*,3*S*,4*R*)-1,3-*O*-Benzylidene-1,2,3,4-nonanetetrol (6). To a suspension of cupper iodide (I) (42.9 g, 225 mmol) in dry THF (560 mL) was added dropwise a solution of *n*-butyllithium (341 mL, 900 mmol, 2.64 M in hexane) at −40 °C under a nitrogen atmosphere. The reaction mixture was stirred for 30 min at −30 °C and then a solution of epoxide **5** (50.0 g, 225 mmol) in dry THF (400 mL) was added dropwise at −40 °C. After being stirred for 3 h at −20 °C, sat. $NaHCO_3$ aq. was added and the product was extracted with EtOAc. The organic layer was washed with brine, dried over anhydrous $MgSO_4$, and concentrated in vacuo to give **6** (61.7 g, 98%) as a white solid: ^1H NMR ($CDCl_3$) δ 7.52–7.50 (m, 2H), 7.42–7.38 (m, 3H), 5.60 (*s*, 1H), 4.28 (dd, 1H, J = 12, 1.8 Hz), 4.05 (1H, dd, J = 12, 1.3 Hz), 3.95–3.88 (m, 2H), 3.71 (dd, 1H, J = 6.6, 1.3 Hz), 3.25 (d, 1H, J = 8.7 Hz), 2.34 (d, 1H, J = 4.5 Hz), 1.73–1.53 (m, 2H), 1.40–1.30 (m, 6H), 0.90 (t, 3H, J = 6.7 Hz); ^{13}C NMR ($CDCl_3$) δ 129.1, 128.3, 126.0, 105.0, 101.2, 81.3, 72.6, 71.2, 63.8, 32.8, 31.8, 25.2, 22.6, 14.0; MS–FAB (*m/z*) 281 $[M + H]^+$; HRMS–FAB (*m/z*) $[M + H]^+$ calcd for $C_{16}H_{25}O_4$, 281.1753, found 281.1658.

(2*R*,3*S*,4*R*)-1,3-*O*-Benzylidene-2-*O*-methanesulfonyl-1,2,3,4-nonanetetrol (7). To a solution of **6** (3.90 g, 13.9 mmol) in dry pyridine (142 mL) was added methansulfonyl chloride (1.05 mL) at −40 °C under a nitrogen atmosphere. The mixture was stirred at the same temperature for 5 h and then gradually warmed to room temperature over 16 h. Azeotropic removal of pyridine by using toluene twice gave a residue that was subjected to column chromatography (*n*-hexane/EtOAc 3:2) to give **7** (4.65 g, 93%) as a white solid: ^1H NMR ($CDCl_3$) δ 7.51–7.48 (m, 2H), 7.42–7.35 (m, 3H), 5.59 (*s*, 1H), 4.99 (d, 1H, J = 1.4 Hz), 4.53 (dd, 1H, J = 13, 1.6 Hz), 4.18 (dd, 1H, J = 13, 1.1 Hz), 3.84–3.75 (m, 2H), 3.19 (*s*, 3H), 1.60–1.27 (m, 8H), 0.90 (t, 3H, J = 6.8 Hz); ^{13}C NMR (CDCl3) δ 129.3, 128.4, 126.1, 101.1, 80.9, 70.4, 70.0, 68.7, 38.7, 33.0, 32.0, 25.1, 22.8, 14.2; MS–FAB (*m/z*) 359 $[M + H]^+$; HRMS–FAB (*m/z*) $[M + H]^+$ calcd for $C_{17}H_{27}O_6S$, 359.1528, found 359.1448.

(2*R*,3*S*,4*R*)-2-*O*-Methanesulfonyl-1,2,3,4-nonanetetrol (8). To a solution of **7** (87.0 mg, 242 μmol) in EtOH (5.0 mL) was added palladium hydroxide ($Pd(OH)_2$) (45 mg). After hydrogenation of the mixture for 16 h at atmospheric pressure, the catalyst was filtered off and the filtrate was concentrated in vacuo to give **8** (65.7 mg, quant) as a white solid: ^1H NMR ($CDCl_3$) δ 5.03–5.00 (m, 1H), 4.02–4.00 (m, 2H), 3.62–3.60 (m, 2H), 3.19 (*s*, 3H), 1.76–1.72 (m, 1H), 1.56–1.28 (m, 7H), 0.90 (t, 3H, J = 6.7 Hz); ^{13}C NMR (CD_3OD) δ 83.8, 74.1, 71.3, 62.6, 38.6, 34.6, 33.2, 26.1, 23.8, 14.4; MS-ESI (*m/z*) 293 $[M + Na]^+$; HRMS–FAB (*m/z*) $[M - OH]^+$ calcd for $C_{10}H_{21}O_5S$, 253.1110, found 253.1069.

(2*S*,3*S*,4*R*)-2-Azido-1,3,4-nonanetriol (9). To a solution of **8** (36.9 mg, 136 μmol) in dry DMF (1.0 mL) was added NaN_3 (17.7 mg, 272 μmol) under a nitrogen atmosphere. The mixture was stirred for 3 h at 95 °C and then quenched with water. After being extracted with ethyl acetate, the organic layer was washed with brine twice, dried over anhydrous Na_2SO_4, and concentrated in vacuo. The residue was purified by column chromatography (CH_2Cl_2/MeOH 15:1) to give **9** (19.5 mg, 66%) as a white solid: ^1H NMR ($CDCl_3$) δ 4.05–3.98 (m, 1H), 3.91–3.74 (m, 3H), 3.71–3.66 (m, 1H), 2.67 (brs 1H), 2.52 (d, 1H, J = 4.4 Hz), 2.20 (brs, 1H), 1.61–1.52 (m, 2H), 1.40–1.31 (m, 6H), 0.91 (t, 3H, J = 6.6 Hz); ^{13}C NMR ($CDCl_3$) δ 74.8, 72.7, 63.3, 61.9, 32.0, 31.9, 25.6, 22.7, 14.2; MS–FAB (*m/z*) 218 $[M + H]^+$; HRMS–FAB (*m/z*) $[M + H]^+$ calcd for $C_9H_{20}N_3O_3$, 218.1505, found 218.1469.

(2*S*,3*S*,4*R*)-2-Azido-3,4-*O*-isopropylidene-1,3,4-nonanetriol (10). To a solution of **9** (4.00 g, 18.4 mmol) in dimethoxypropane (73 mL) was added a catalytic amount of *p*-toluenesulfonic acid monohydrate (175 mg, 92 μmol) at 0 °C. Stirring was continued for 2 h at room temperature. The mixture was

quenched with MeOH and then stirred for 1 h at room temperature. Removal of the solvent gave a residue, which was purified by column chromatography (*n*-hexane/EtOAc 4:1) to give **10** (3.61 g, 75%) as a colorless oil: ^{1}H NMR ($CDCl_3$) δ 4.21−4.16 (m, 1H), 4.02−3.95 (m, 2H), 3.90−3.84 (m, 1H), 3.50−3.45 (m, 1H), 2.11 (t, 1H, J = 5.6 Hz), 1.63−1.54 (m, 2H), 1.43 (s, 3H), 1.40−1.34 (m, 9H), 0.91(t, 3H, J = 6.9 Hz); ^{13}C NMR ($CDCl_3$) δ 108.6, 77.8, 76.6, 63.9, 61.2, 31.8, 29.4, 28.0, 26.2, 25.6, 22.6, 14.0; MS-ESI (*m/z*) 280 $[M + Na]^+$; HRMS−FAB (*m/z*) $[M + H]^+$ calcd for $C_{12}H_{24}N_3O_3$, 258.1818, found 258.1737.

(2*S*,3*S*,4*R*)-2-Azido-3,4-*O*-isopropylidene-1-*O*-(2,3,4,6-tetra-*O*-benzyl-α-D-galactosyl)-1,3,4-nonanetriol (12a). To a suspension of **10** (100 mg, 389 μmol), **11b** (428 mg, 710 μmol), and molecular sieves 4Å (powder, 340 mg) in dry toluene (3.4 mL) and dry DMF (1.4 mL) was added tetra-*n*-butylammonium bromide (*n*-Bu_4NBr) (377 mg, 1.17 mmol) under a nitrogen atmosphere. The reaction mixture was stirred for 5 days at room temperature. The mixture was quenched with MeOH (0.1 mL) and stirred for 1 h at room temperature. After being passed through Celite, the filtrate was washed with sat. $NaHCO_3$ aq. and brine and then dried over anhydrous $MgSO_4$. Removal of the solvent gave a residue, which was purified by column chromatography (*n*-hexane/EtOAc 7:1) to give **12a** (206 mg, 68%) as a colorless oil: ^{1}H NMR ($CDCl_3$) δ 7.40−7.26 (m, 20H), 4.97−4.93 (m, 2H), 4.87−4.79 (m, 2H), 4.74−4.70 (m, 2H), 4.57 (d, 1H, J = 12 Hz), 4.49 (d, 1H, J = 12 Hz), 4.41 (d, 1H, J = 12 Hz), 4.10−3.94 (m, 7H), 3.75−3.70 (m, 1H), 3.56−3.44 (m, 3H), 1.62−1.49 (m, 2H), 1.40−1.26 (m, 12H), 0.91 (t, 3H, J = 6.6 Hz); ^{13}C NMR ($CDCl_3$) δ 139.3, 139.1, 138.5, 128.8, 128.8, 128.7, 128.7, 128.7, 128.2, 128.1, 128.1, 128.0, 127.9, 108.6, 99.3, 79.1, 78.2, 77.0, 75.8, 75.7, 75.2, 73.9, 73.8, 73.3, 70.3, 70.0, 69.6, 60.3, 32.3, 29.7, 28.6, 26.7, 26.2, 23.0, 14.5; MS-ESI (*m/z*) 803 $[M + Na]^+$; HRMS−FAB (*m/z*) $[M - N_2]^+$ calcd for $C_{46}H_{57}NO_8$, 751.4084, found 751.4134.

(2*S*,3*S*,4*R*)-2-Azido-3,4-*O*-isopropylidene-1-*O*-(2,3,4,6-tetra-*O*-benzyl-β-D-galactosyl)-1,3,4-nonanetriol (12b). To a suspension of **10** (100 mg, 389 μmol), **11a** (285 mg, 524 μmol), and molecular sieves 4Å (powder, 400 mg) in dry $CHCl_3$ (5 mL) was added $BF_3{\cdot}Et_2O$ (47 μL, 368 μmol) in dry $CHCl_3$ (2 mL) at −50 °C under a nitrogen atmosphere. After stirring was continued for 14 h at the same temperature, the workup in the same manner for the reaction of **10** and **11b** provided **12a** (173 mg, 57%) along with **12b** (76 mg, 25%) as a colorless oil. **Data for 12b**: ^{1}H NMR ($CDCl_3$) δ 7.38−7.23 (m, 20H), 4.96−4.90 (m, 2H), 4.83−4.61 (m, 4H), 4.46−4.39 (m, 3H), 4.12−4.04 (m, 2H), 3.92−3.77 (m, 4H), 3.62−3.51 (m, 5H), 1.64−1.23 (m, 14H), 0.91 (t, 3H, J = 6.3 Hz); ^{13}C NMR ($CDCl_3$) δ 138.9, 138.6, 138.5, 137.9, 128.5, 128.4, 128.3, 128.3, 128.2, 128.0, 127.9, 127.8, 127.6, 127.6, 127.6, 108.3, 104.1, 82.2, 79.7, 77.8, 75.8, 75.3, 74.6, 73.6, 73.6, 73.5, 73.1, 70.6, 68.7, 60.5, 31.9, 29.4, 28.2, 26.1, 25.7, 22.6, 14.1; MS-ESI (*m/z*) 803 $[M + Na]^+$; HRMS−FAB (*m/z*) $[M - N_2]^+$ calcd for $C_{46}H_{57}NO_8$, 751.4084, found 751.4005.

(2*S*,3*S*,4*R*)-2-Amino-3,4-*O*-isopropylidene-1-*O*-(2,3,4,6-tetra-*O*-benzyl-α-D-galactosyl)-1,3,4-nonanetriol (13). To a solution of **12a** (2.58 g, 3.31 mmol) in EtOH (260 mL) was added palladium on calcium carbonate poisoned with lead (Lindlar catalyst) (2.60 g). After hydrogenation was carried out for 16 h at atmospheric pressure, the catalyst was filtered off and the filtrate was concentrated in vacuo to give **13** (2.46 g, quant) as a colorless oil: ^{1}H NMR ($CDCl_3$) δ 7.40−7.25 (m, 20H), 4.96−4.92 (m, 2H), 4.84−4.64 (m, 4H), 4.58 (d, 1H, J = 11 Hz), 4.50 (d, 1H, J = 12 Hz), 4.41 (d, 1H, J = 12 Hz), 4.13−3.86 (m, 6H), 3.58−3.51 (m, 2H), 3.42−3.37 (m, 1H), 3.07−3.01 (m, 1H), 1.65−1.20 (m, 14H), 0.90 (t, 3H, J = 5.6 Hz); ^{13}C NMR ($CDCl_3$) δ 138.8, 138.7, 138.6, 138.0, 128.4, 128.4, 128.2, 127.8, 127.8, 127.7, 127.6, 127.6, 127.5, 127.4, 107.9, 99.0, 79.1, 79.0, 77.9, 74.9, 74.8, 73.5, 73.3, 73.0, 72.4, 69.5, 69.0, 50.7, 31.9, 29.8, 28.3, 26.0, 25.9, 22.6, 14.1; MS-ESI (*m/z*) 754 $[M + H]^+$; HRMS−FAB (*m/z*) $[M + H]^+$ calcd for $C_{46}H_{60}NO_8$, 754.4319, found 754.4194.

(2*S*,3*S*,4*R*)-3,4-*O*-Isopropylidene-1-*O*-(2,3,4,6-tetra-*O*-benzyl-α-D-galactosyl)-2-tetracosanoylamino-1,3,4-nonanetriol (14). To a suspension of *n*-tetracosanoic acid (1.22 g, 3.31 mmol) in DMF (90 mL) and CH_2Cl_2 (210 mL) were added 1-ethyl-3-(3-dimethylaminopropyl) carbodiimide hydrochloride (EDCI) (761 mg, 3.97 mmol) and 1-hydroxybenzotriazol (HOBt) (536 mg, 3.97 mmol) at 0 °C. After the mixture was stirred for 30 min at room temperature, **13** (2.46 g, 3.26 mmol) and *i*-Pr_2NEt (1.38 mL, 7.97 mmol) in CH_2Cl_2 (120 mL) were added and stirred for 16 h at 30 °C. The mixture was diluted with EtOAc/Et_2O (4:1) and sat. $NaHCO_3$ aq., and then the organic layer was separated and washed with 1 M HCl aq. and brine, and dried over anhydrous $MgSO_4$. Removal of the solvent gave a residue, which was purified by column chromatography (*n*-hexane/EtOAc 3:1) to give **14** (3.25 g, 89%) as a white solid: ^{1}H NMR ($CDCl_3$) δ 7.41−7.24 (m, 20H), 6.28 (d, 1H, J = 8.4 Hz), 4.95−4.90 (m, 2H), 4.83−4.73 (m, 2H), 4.75 (d, 1H, J = 12 Hz), 4.66 (d, 1H, J = 11 Hz), 4.58 (d, 1H, J = 12 Hz), 4.49 (d, 1H, J = 12 Hz), 4.38 (d, 1H, J = 12 Hz), 4.13−4.03 (m, 4H), 3.98 (t, 1H, J = 6.2 Hz), 3.93−3.90 (m, 3H), 3.63−3.53 (m, 2H), 3.39 (dd, 1H, J = 9.4, 5.7 Hz), 2.08−1.95 (m, 2H), 1.55−1.25 (m, 50H), 1.40 (s, 3H), 1.32 (s, 3H), 0.90−0.84 (m, 6H); ^{13}C NMR ($CDCl_3$) δ 172.4, 138.7, 138.4, 137.6, 128.5, 128.4, 128.4, 128.4, 128.3, 128.0, 127.9, 127.8, 127.7, 127.6, 127.5, 107.8, 99.9, 79.0, 77.8, 76.8, 75.5, 74.8, 74.7, 73.6, 73.5, 73.0, 70.8, 69.9, 69.6, 48.7, 36.8, 31.9, 31.8, 29.7, 29.7, 29.6, 29.5, 29.4, 29.3, 28.9, 28.2, 26.2, 26.0, 25.7, 22.7, 22.6, 14.1, 14.1; MS−FAB 1105 $[M + H]^+$; HRMS−FAB (*m/z*) $[M + H]^+$ calcd for $C_{70}H_{106}NO_9$, 1104.7868, found 1104.7589.

(2*S*,3*S*,4*R*)-1-*O*-(α-D-Galactosyl)-2-tetracosanoylamino-1,3,4-nonanetriol (1b). To a solution of **14** (89 mg, 81 μmol) in MeOH (1.0 mL) and CH_2Cl_2 (5.0 mL) was added 4 M HCl aq. in dioxane (100 μL) at 0 °C. After the mixture was stirred for 2 h at room temperature, evaporation of the solvent gave a residue, which was purified by column chromatography (CH_2Cl_2/MeOH 30:1) to give the product by which the acetal group was deprotected. To a solution of the obtained diol in MeOH (3.0 mL) and $CHCl_3$ (1.0 mL) was added $Pd(OH)_2$ (25 mg). After hydrogenation was carried out for 3 h at atmospheric pressure, the catalyst was filtered off and the filtrate was evaporated to give **1b** (46 mg, 84%) as colorless crystals, mp 142−145 °C (recrystallized from EtOH/H_2O 10:1); $[\alpha]^{30}_D$ +53.9 (*c* 0.5, pyridine); ^{1}H NMR ($CDCl_3$/CD_3OD 3:1) δ 4.71 (d, 1H, J = 3.8 Hz), 4.01−3.98 (m, 1H), 3.74−3.65 (m, 2H), 3.62−3.45 (m, 6H), 3.35−3.31 (m, 2H), 2.00 (t, 2H, J = 7.6 Hz), 1.51−1.01 (m, 50H), 0.71−0.67 (m, 6H); ^{13}C NMR (pyridine-d_5) δ 173.8, 102.1, 77.3, 73.6, 73.0, 72.2, 71.6, 70.9, 69.2, 63.2, 52.0, 37.4, 34.9, 33.0, 32.7, 30.6, 30.6, 30.5, 30.4, 30.4, 30.3, 30.2, 27.0, 26.7, 23.6, 23.5, 14.8; MS−FAB (*m/z*) 704 $[M + H]^+$; HRMS−FAB (*m/z*) $[M + H]^+$ calcd for $C_{39}H_{78}NO_9$, 704.5677, found 704.5687. Anal. Calcd for $C_{39}H_{77}NO_9{\cdot}H_2O$: C, 64.87; H, 11.03; N, 1.94. Found: C, 64.71; H, 10.88; N, 1.94.

Acknowledgment. We thank Mr. N. Takemoto, Ms. M. Akabane, Mr. N. Ogou, and Ms. J. Futamura for their contribution to the synthesis of related analogues. We also thank Drs. T. Nishihara and G. Nakayama for their support and encouragement throughout this study.

Note Added after ASAP Publication. As the result of a production error, the formatting of the compound names in the Experimental Section was inconsistent in the version published ASAP February 16, 2005. These have been corrected, and the solvent was changed in the synthesis of **12b**. The corrected version was published February 18, 2005.

Supporting Information Available: ^{1}H and/or ^{13}C NMR spectra of **1b**, **3**−**10**, **12a**, **12b**, **13**, and **14**. This material is available free of charge via the Internet at http://pubs.acs.org.

JO048151Y

Stimulation of Host NKT Cells by Synthetic Glycolipid Regulates Acute Graft-versus-Host Disease by Inducing Th2 Polarization of Donor T Cells[1]

Daigo Hashimoto,* Shoji Asakura,* Sachiko Miyake,† Takashi Yamamura,† Luc Van Kaer,‡ Chen Liu,§ Mitsune Tanimoto,* and Takanori Teshima[2]*¶

NKT cells are a unique immunoregulatory T cell population that produces large amounts of cytokines. We have investigated whether stimulation of host NKT cells could modulate acute graft-vs-host disease (GVHD) in mice. Injection of the synthetic NKT cell ligand α-galactosylceramide (α-GalCer) to recipient mice on day 0 following allogeneic bone marrow transplantation promoted Th2 polarization of donor T cells and a dramatic reduction of serum TNF-α, a critical mediator of GVHD. A single injection of α-GalCer to recipient mice significantly reduced morbidity and mortality of GVHD. However, the same treatment was unable to confer protection against GVHD in NKT cell-deficient CD1d knockout (CD1d$^{-/-}$) or IL-4$^{-/-}$ recipient mice or when STAT6$^{-/-}$ mice were used as donors, indicating the critical role of host NKT cells, host production of IL-4, and Th2 cytokine responses mediated by donor T cells on the protective effects of α-GalCer against GVHD. Thus, stimulation of host NKT cells through administration of NKT ligand can regulate acute GVHD by inducing Th2 polarization of donor T cells via STAT6-dependent mechanisms and might represent a novel strategy for prevention of acute GVHD. *The Journal of Immunology,* 2005, 174: 551–556.

Allogeneic hemopoietic stem cell transplantation (HSCT)[3] cures various hematologic malignant tumors, bone marrow (BM) failures, and congenital metabolic disorders. Emerging evidence suggests that allogeneic HSCT is also useful for treatment of other diseases, including solid tumors and autoimmune diseases (1, 2). However, graft-vs-host disease (GVHD) is a major obstacle that precludes wider application of allogeneic HSCT. The pathophysiology of acute GVHD is complex, involving 1) donor T cell responses to the host alloantigens expressed by host APCs activated by conditioning regimens (i.e., irradiation and/or chemotherapy), and 2) dysregulation of inflammatory cytokine cascades, leading to further T cell expansion and induction of cytotoxic T cell responses (3).

CD4$^+$ helper T cells can be divided into two distinct subpopulations: Th1 and Th2 cells (4). Th1 cells produce IFN-γ and IL-2, whereas Th2 cells produce IL-4, IL-5, and IL-13. Although the role of Th1 and Th2 cytokines in the pathophysiology of acute GVHD is complex and controversial (5–8), Th1 polarization of donor T cells predominantly plays a role in inducing the "cytokine storm" that is seen in several models of acute GVHD (3, 9), whereas Th2 polarization mostly suppresses inflammatory cascades and reduces acute GVHD (10–12). Many properties of dendritic cells (DCs), including the type of signal, the duration of activation, the ratio of DCs to T cells, and the DC subset that presents the Ag, influence the differentiation of naive CD4$^+$ T cells into Th1 or Th2 cells (13). The cytokines that are present during the initiation of the immune responses at the time when the TCR engages with MHC/peptide Ags are critically important for Th cell differentiation (14).

NKT cells are a distinct subset of lymphocytes characterized by expression of surface markers of NK cells together with a TCR. Although the NKT cell population exhibits considerable heterogeneity with regard to phenotypic characteristics and functions (15), the major subset of murine NKT cells expresses a semi-invariant TCR, Vα14-Jα18, in combination with a highly skewed set of Vβs, mainly Vβ8 (16). NKT cells can be activated via their TCR by glycolipid Ags presented by the nonpolymorphic MHC class I-like molecule CD1d expressed by APCs (17). Stimulation of NKT cells rapidly induces secretion of large amounts of IFN-γ and IL-4, thereby influencing the Th1/Th2 balance of conventional CD4$^+$ T cell responses (18). In particular, NKT cells are considered an important early source of IL-4 for the initiation of Th2 responses (19, 20), although these cells are not absolutely required for the induction of Th2 responses (21–23). NKT cells are absent in CD1d knockout (CD1d$^{-/-}$) mice because of defects in their thymic positive selection, which requires CD1d expression on hemopoietic cells, probably double-positive thymocytes (24, 25).

Considering the critical role of cytokines in the development of acute GVHD, we investigated the role of host NKT cells in an experimental model of GVHD, using synthetic NKT cell ligands,

*Biopathological Science, Okayama University Graduate School of Medicine and Dentistry, Okayama, Japan; †Department of Immunology, National Institute of Neuroscience, Tokyo, Japan; ‡Department of Microbiology and Immunology, Vanderbilt University School of Medicine, Nashville, TN 37232; §Department of Pathology, University of Florida College of Medicine, Gainesville, FL 32610; and ¶Center for Cellular and Molecular Medicine, Kyushu University Hospital, Fukuoka, Japan

Received for publication August 6, 2004. Accepted for publication October 15, 2004.

The costs of publication of this article were defrayed in part by the payment of page charges. This article must therefore be hereby marked *advertisement* in accordance with 18 U.S.C. Section 1734 solely to indicate this fact.

[1] This work was supported by research funds from the Ministry of Education, Culture, Sports, Science and Technology Grant 15591007 (to T.T.), by the Health and Labor Science Research Grants for Clinical Research for Evidence Based Medicine (to T.T.), by grants from the Ministry of Health, Labour, and Welfare of Japan (to T.Y.), by the Organization for Pharmaceutical Safety and Research (to T.Y.), and by a grant-in-aid for cancer research from the Fukuoka Cancer Society.

[2] Address correspondence and reprint requests to Dr. Takanori Teshima, Center for Cellular and Molecular Medicine, Kyushu University Hospital, 3-1-1 Maidashi, Higashi-ku, Fukuoka 812-8582, Japan. E-mail address: tteshima@cancer.med.kyushu-u.ac.jp

[3] Abbreviations used in this paper: HSCT, hemopoietic stem cell transplantation; BM, bone marrow; GVHD, graft-vs-host disease; DC, dendritic cell; α-GalCer, α-galactosylceramide; BMT, bone marrow transplantation; TBI, total body irradiation; TCD, T cell depletion; LN, lymph node; WT, wild type.

0022-1767/05/$02.00

α-galactosylceramide (α-GalCer) (26), a glycolipid originally purified from a marine sponge, and its analog, OCH (27). Our findings indicate that stimulation of host NKT cells with NKT ligands can modulate acute GVHD.

Materials and Methods

Mice

Female C57BL/6 (B6, H-2^b) and BALB/c (H-2^d) mice were purchased from Charles River Japan. IL-$4^{-/-}$ B6 and STAT$6^{-/-}$ BALB/c mice were purchased from The Jackson Laboratory. CD1$d^{-/-}$ B6 mice were established by specific deletion of the CD1d1 gene segment (22). Mice, between 8 and 16 wk of age, were maintained in a specific pathogen-free environment and received normal chow and hyperchlorinated drinking water for the first 3 wk post-bone marrow transplantation (BMT). All experiments involving animals were performed under the auspices of the Institutional Animal Care and Research Advisory Committee at the Department of Animal Resources, Okayama University Advanced Science Research Center.

Bone marrow transplantation

Mice were transplanted according to a standard protocol described previously (28). Briefly, B6 mice received lethal total body irradiation (TBI; x-ray), split into two doses separated by 6.5 h to minimize gastrointestinal toxicity. Recipient mice were injected with 5×10^6 BM cells plus 5×10^6 spleen cells from either syngeneic (B6) or allogeneic (BALB/c) donors. T cell depletion (TCD) of donor BM cells was performed using anti-CD90 MicroBeads and the AutoMACS system (Miltenyi Biotec) according to the manufacturer's instructions. Donor cells were resuspended in 0.25 ml of HBSS (Invitrogen Life Technologies) and injected i.v. into recipients on day 0. Survival was monitored daily. The degree of systemic acute GVHD was assessed weekly by a scoring system incorporating five clinical parameters: weight loss, posture (hunching), activity, fur texture, and skin integrity, as described (29).

Glycolipids

α-GalCer, (2S,3S,4R)-1-*O*-(α-D-galactopyranosyl)-2-(*N*-hexacosanoylamino)-1,3,4-octadecanetriol (KRN7000), was synthesized and provided by Kirin Brewery Company (30). A homologue of α-GalCer, OCH, was selected from a panel of synthesized α-GalCer analogues by replacing the sugar moiety and/or truncating the aliphatic chains, because of its ability to stimulate enhanced IL-4 and reduced IFN-γ production by NKT cells, as previously described (27, 31). BMT recipient mice were injected i.p. with α-GalCer or OCH (100 μg/kg) immediately after BMT on day 0. Mice from the control groups received the diluent only.

Flow cytometric analysis

mAbs used were FITC- or PE-conjugated anti-mouse CD4, H-$2K^b$, and H-$2K^d$ (BD Pharmingen). Cells were preincubated with 2.4G2 mAb (rat anti-mouse FcγR) for 10 min at 4°C to block nonspecific binding of labeled Abs, and then were incubated with the relevant mAbs for 15 min on ice. Finally, cells were washed twice with 0.2% BSA in PBS and fixed. After lysis of RBCs with FACS lysing solution (BD Pharmingen), cells were analyzed using a FACSCalibur flow cytometer (BD Biosciences). 7-Amino-actinomycin D (BD Pharmingen)-positive cells (i.e., dead cells) were excluded from the analysis. Fluorochrome-conjugated irrelevant IgG were used as negative controls. At least 5000 live events were acquired for analysis.

Cell cultures

Mesenteric lymph nodes (LNs) and spleens were removed from animals 6 days after BMT and four to six mesenteric LNs or spleens from each experimental group were combined. Numbers of cells were normalized for T cells and were cultured in complete DMEM (Invitrogen Life Technologies) supplemented with 10% FCS, 50 U/ml penicillin, 50 μg/ml streptomycin, 2 mM L-glutamine, 1 mM sodium pyruvate, 0.1 mM nonessential amino acids, 0.02 mM 2-ME, and 10 mM HEPES in wells of a 96-well flat-bottom plate, at a concentration of 5×10^4 T cells/well with 1×10^5 irradiated (20 Gy) peritoneal cells harvested from naive B6 (allogeneic) animals, or with 5 μg/ml plate-bound anti-CD3ε mAbs (BD Pharmingen) and 2 μg/ml anti-CD28 mAbs (BD Pharmingen). Forty-eight hours after the initiation of culture, supernatants were collected for the measurement of cytokine levels.

ELISA

ELISA was performed according to the manufacturer's protocols (R&D Systems) for measurement of IFN-γ, IL-4, and TNF-α levels, as described previously (32). Samples were obtained from culture supernatant and blood from retro-orbital plexus, diluted appropriately, and run in duplicate. Plates were read at 450 nm using a microplate reader (Bio-Rad). The sensitivity of the assays was 31.25 pg/ml for IFN-γ, 7.6 pg/ml for IL-4, and 23.4 pg/ml for TNF-α.

Histology

Formalin-preserved livers and small and large bowels were embedded in paraffin, cut into 5-μm-thick sections, and stained with H&E for histological examination. Slides were coded without reference to prior treatment and examined in a blinded fashion by a pathologist (C. Liu). A semiquantitative scoring system was used to assess the following abnormalities known to be associated with GVHD, as previously described (33): 0, normal; 0.5, focal and rare; 1.0, focal and mild; 2.0, diffuse and mild; 3.0, diffuse and moderate; and 4.0, diffuse and severe. Scores were added to provide a total score for each specimen. After scoring, the codes were broken and data were compiled. Pathological GVHD scores of intestine are the sum of scores for small bowel and colon.

Statistical analysis

Mann-Whitney *U* test was applied for the analysis of cytokine data and clinical scores. We used the Kaplan-Meier product limit method to obtain survival probability, and the log-rank test was applied for comparing survival curves. Differences in pathological scores between the α-GalCer-treated group and the diluent-treated group were examined by two-way ANOVA. We defined $p < 0.05$ as statistically significant.

Results

Administration of α-GalCer stimulates lethally irradiated mice to produce IFN-γ and IL-4

We first determined whether administration of synthetic NKT ligands such as α-GalCer and OCH can stimulate heavily irradiated mice to produce cytokines. B6 mice were given 13 Gy TBI and were injected i.p. with α-GalCer, OCH, or diluent 2 h after TBI. Six hours later, blood samples were obtained, and serum samples were prepared for measurement of IFN-γ and IL-4. TBI alone or BMT itself did not stimulate diluent-treated mice to produce IFN-γ or IL-4 (Fig. 1). Administration of α-GalCer increased serum levels of IFN-γ and IL-4, even in mice receiving TBI. However, serum levels of IFN-γ were much less in irradiated mice than in unirradiated mice. By contrast, the ability of irradiated mice to produce IL-4 to α-GalCer was maintained for 48 h after irradiation. Serum levels of IFN-γ and IL-4 in response to α-GalCer were not altered when irradiated wild-type (WT) mice were injected with 5×10^6 BM cells and 5×10^6 spleen cells isolated from allogeneic (BALB/c) donors. Furthermore, these cytokine responses were not observed when α-GalCer was injected into irradiated NKT cell-deficient CD1$d^{-/-}$ mice with or without BMT. These results suggest that host NKT cells that survive for at least 48 h after irradiation, rather than from infused donor cells, are critically involved in the production of these cytokines in response to glycolipids. Irradiation appears to impair the ability of mice to produce IFN-γ while preserving IL-4 production in response to α-GalCer. Similar cytokine profiles were observed when OCH was administered (data not shown).

Administration of α-GalCer to recipients polarizes donor T cells toward Th2 cytokine production after allogeneic BMT

Induction of GVHD fundamentally depends upon donor T cell responses to host alloantigens. We next evaluated the effect of glycolipid administration on donor T cell responses after allogeneic BMT in a well-characterized murine model of acute GVHD (BALB/c→ B6) directed against both MHC and multiple minor histocompatibility Ags. Lethally irradiated B6 mice were transplanted with 5×10^6 BM cells and 5×10^6 spleen cells from